

# Exclusive production of quarkonia pairs in collinear factorization framework

Marat Siddikov, Iván Schmidt

*Departamento de Física, Universidad Técnica Federico Santa María,  
y Centro Científico - Tecnológico de Valparaíso, Casilla 110-V, Valparaíso, Chile*

In this paper we analyze the exclusive photoproduction of heavy quarkonia pairs in the collinear factorization framework. We evaluate the amplitude of the process for  $J/\psi - \eta_c$  quarkonia pair in the leading order of the strong coupling  $\alpha_s$ , and express it in terms of generalized parton distributions (GPDs) of gluons in the proton. We made numerical estimates in the kinematics of the Electron Ion Collider, and found that in the photoproduction regime, when the virtuality of the photon is much smaller than the quarkonia mass, the cross-section of the process is sufficiently large for experimental studies. We demonstrate that the study of this channel can complement existing studies of gluon GPDs from other channels.

## I. INTRODUCTION

Understanding the proton structure presents one of the central problems in high energy physics. Usually this structure is parametrized in terms of partonic and multipartonic distributions of different flavors. In view of the nonperturbative nature of strong interactions, it is not possible to evaluate these distributions theoretically from first principles, and thus we have to extract them from experimental data. For exclusive processes, the amplitudes are usually controlled by the Generalized Parton Distributions (GPDs) of the target [1–6]. However, extraction of the GPDs from experimental data suffers from a number of technical challenges, and at present inevitably requires the use of model assumptions, even for Compton scattering and meson production, which are considered as references in nucleon tomography [7]. Many observables might obtain simultaneously contributions of GPDs with different helicity and flavor states, albeit with different, process-dependent weights. For this reason, the extraction of partonic distributions of individual flavors inevitably requires analysis of multiple channels, and thus the extension of the number of possible channels for study of GPDs is strongly desired [87–90]. Recently a new class of  $2 \rightarrow 3$  processes has been suggested in the literature [8–17, 85, 86], as potential new probes, which should complement existing studies, provide more stringent constraints on existing phenomenological models and in this way diminish theoretical uncertainty. Most of these studies focused on the production of light mesons and photons. Such processes are dominated by quark GPDs (both in chiral odd and chiral even sectors). A factorization for such processes has been proven in the kinematics when the relative transverse momenta of the produced hadrons and photon ( $\sim$ pairwise invariant masses) are large enough to avoid soft final-state interactions [18, 19].

In these analyses special attention should be paid to the extraction of gluon GPDs. Since the gluons do not couple directly to photons, they contribute to many processes only as higher order corrections, which adversely affects the precision of the extracted gluon GPDs. However, knowledge of the gluon GPDs is important for solving many puzzles (see [1–6] for overview). The best channel for the study of gluon GPDs is the production of heavy quarkonia. Due to the expected smallness of intrinsic heavy parton densities, the process gets a dominant contribution from gluon GPDs, which might therefore be studied in detail. The heavy mass of quarkonia plays the role of a natural hard scale in the problem [20, 21], relaxing the conditions on other kinematic variables and potentially opening the possibility to use perturbative methods even in photoproduction regime. A modern NRQCD framework allows to incorporate systematically various perturbative corrections [22–33]. The use of single quarkonia production for constraining the gluon GPDs has been discussed in detail in [34–37], and the coefficient functions have been evaluated, taking into account next-to-leading order and some higher twist corrections. However, the amplitude of this process provides information only about GPDs convoluted with process-dependent coefficient functions, and, as mentioned earlier, an inversion of the procedure might be impossible, especially when the complicated structure of higher-order corrections is taken into account. For this reason it is important to complement the analysis with data from other channels. A natural and straightforward extension of these studies is the production of multiple quarkonia (*e.g.* heavy quarkonia pairs). Such processes have been the subject of theoretical studies since the early days of QCD [38–41], and recently got renewed interest due to the forthcoming launch of high-luminosity accelerator facilities, as well as being a potential gateway for the study of all-heavy tetraquarks, which might be molecular states of quarkonia pairs [42–52].

Previously, the exclusive production of quarkonia pairs has been studied for  $J/\psi J/\psi$  production, which might proceed only via a two-photon mechanism,  $\gamma\gamma \rightarrow M_1 M_2$  [53–58] due to  $C$ -parity constraints and thus cannot be used for studies of gluon GPDs. Recently we analyzed the production of quarkonia pairs with opposite  $C$ -parities, which proceeds via photon-pomeron fusion and thus have larger cross-sections [59]. However, our study was realized in the framework of the Color Glass Condensate approach and relied on an underlying eikonal picture, which is valid in the small- $x$  domain. At smaller energies, as well as in the kinematics of large photon virtuality  $Q^2$ , the assumptions of this

picture are not well-justified, and it makes sense to analyze this process in the complementary collinear factorization approach, which is expected to give reasonable predictions in this kinematics and give access to the aforementioned gluon GPDs of the target. This kinematic regime might be studied in low-energy electron-proton collisions at the forthcoming Electron Ion Collider (EIC) [60–63].

The paper is structured as follows. Below, in Section II, we discuss in detail the kinematics of the process and the framework for the evaluation of the amplitude of the process. In Section III we present our numerical estimates for the cross-sections, in EIC kinematics. Finally, in Section IV we draw conclusions.

## II. EXCLUSIVE PHOTOPRODUCTION OF MESON PAIRS

Previously, the exclusive production of *light* meson pairs was analyzed in Bjorken kinematics in [64–68], with the additional constraint that the invariant mass of meson pair should be large. There it was demonstrated that the amplitude of that process might be represented as a convolution of the quark and gluon GPDs of the target, with novel 2-meson distribution amplitudes. However, the extension of those results to quarkonia pairs is not straightforward, since quarkonia masses and the invariant mass  $M_{12}$  are very large, so the Bjorken regime ( $Q \gg M_{12}$ ) is achieved in the kinematics where the cross-section is negligibly small. For this reason, it makes sense to analyze the quarkonia pair production by treating the heavy mass of the quark and the photon virtuality  $Q$  as two independent hard scales, with the photoproduction ( $Q \ll M_{12}$ ) and Bjorken ( $Q \gg M_{12}$ ) regimes as limiting cases. In the following subsection II A we discuss in detail the kinematics of the process, and in subsection II B we discuss the evaluation of the amplitudes in the collinear factorization approach, and their relation to the target gluon GPDs.

### A. Kinematics of the process

In order to facilitate the comparison with experimental data, in what follows we will present our results in the frame whose axis  $z$  coincides with the photon-proton collision axis, so the light-cone decomposition of the momenta is given by

$$q = \left( -\frac{Q^2}{2q^-}, q^-, \mathbf{0}_\perp \right), \quad q^- = E_\gamma + \sqrt{E_\gamma^2 + Q^2} \quad (1)$$

$$P = \left( P^+, \frac{m_N^2}{2P^+} \mathbf{0}_\perp \right), \quad P^+ = E_p + \sqrt{E_p^2 - m_N^2} \quad (2)$$

$$p_a = \left( \frac{M_a^\perp}{2} e^{-y_a}, M_a^\perp e^{y_a}, \mathbf{p}_a^\perp \right), \quad a = 1, 2, \quad (3)$$

$$M_a^\perp \equiv \sqrt{M_a^2 + (\mathbf{p}_a^\perp)^2}, \quad (4)$$

where  $q$  is the (virtual) photon momentum,  $P$  and  $P'$  are the momenta of the proton before and after the collision, and  $p_1, p_2$  are the 4-momenta of the produced heavy quarkonia; the latter are expressed in terms of the rapidities and transverse momenta ( $y_a, \mathbf{p}_a^\perp$ ) of these heavy mesons. This frame allows for straightforward analysis down to the photoproduction limit ( $Q \rightarrow 0$ ). The relation of this frame to the so-called symmetric frame [2, 3, 67, 69–73], which is used for the analysis in Bjorken kinematics ( $Q \rightarrow \infty$ ), is discussed in detail in Appendix A. In the limit  $Q \rightarrow 0$ , this frame, up to a trivial longitudinal boost, coincides with the frame used in earlier studies of exclusive photoproduction  $\gamma p \rightarrow \gamma Mp$  [8–17]. In this frame, the polarization vectors of the longitudinally and transversely polarized photons are chosen respectively as <sup>1</sup>

$$\varepsilon_L = \left( \frac{Q}{q^-}, 0, \mathbf{0}_\perp \right), \quad \varepsilon_T^{(\pm)} = \left( 0, 0, \frac{1}{\sqrt{2}}, \pm \frac{i}{\sqrt{2}} \right). \quad (5)$$

We also will use the notations

$$\Delta = P' - P = q - p_1 - p_2 = \left( \Delta^+, \Delta^-, \mathbf{\Delta}^\perp \right), \quad (6)$$

---

<sup>1</sup> We've chosen the longitudinal vector in the light-cone gauge, so the contribution of the longitudinal photons in the  $ep$  amplitude might be reinterpreted as instantaneous part of the photon propagator. The results will not change under any redefinition of polarization vectors  $\varepsilon_\mu(q) \rightarrow \varepsilon_\mu(q) + \text{const } q_\mu$  in view of the Ward identity (in this problem it remains valid even for offshell photons, since all amplitudes with an omitted photon vertex vanish due to  $C$ -parity).

$$\Delta^+ = -\frac{Q^2}{2q^-} - \frac{M_1^\perp e^{-y_1}}{2} - \frac{M_2^\perp e^{-y_2}}{2}, \quad \Delta^- = q^- - M_1^\perp e^{y_1} - M_2^\perp e^{y_2}, \quad \Delta_\perp = -\mathbf{p}_1^\perp - \mathbf{p}_2^\perp \quad (7)$$

for the 4-vector of momentum transfer to the proton and its components, and the notation  $t$  for its square,

$$\begin{aligned} t = \Delta^2 &= -\left(q^- - M_1^\perp e^{y_1} - M_2^\perp e^{y_2}\right) \left(\frac{Q^2}{q^-} + M_1^\perp e^{-y_1} + M_2^\perp e^{-y_2}\right) - (\mathbf{p}_1^\perp + \mathbf{p}_2^\perp)^2 \\ &= -Q^2 + M_1^2 + M_2^2 - q^- (M_1^\perp e^{-y_1} + M_2^\perp e^{-y_2}) + \frac{Q^2}{q^-} (M_1^\perp e^{y_1} + M_2^\perp e^{y_2}) \\ &\quad + 2(M_1^\perp M_2^\perp \cosh \Delta y - \mathbf{p}_1^\perp \cdot \mathbf{p}_2^\perp). \end{aligned} \quad (8)$$

After the interaction, the 4-momentum of the proton is given by

$$P' = P + \Delta = \left(q^- + \frac{m_N^2}{2P^+} - M_1^\perp e^{y_1} - M_2^\perp e^{y_2}, P^+ - \frac{Q^2}{2q^-} - \frac{M_1^\perp e^{-y_1} + M_2^\perp e^{-y_2}}{2}, -\mathbf{p}_1^\perp - \mathbf{p}_2^\perp\right), \quad (9)$$

and the onshellness condition  $(P + \Delta)^2 = m_N^2$  allows to get an additional constraint

$$q^- P^+ = P^+ (M_1^\perp e^{y_1} + M_2^\perp e^{y_2}) - \frac{m_N^2 + t}{2} + \frac{m_N^2}{4P^+} \left(M_1^\perp e^{-y_1} + M_2^\perp e^{-y_2} + \frac{Q^2}{q^+}\right). \quad (10)$$

Solving the Equation (10) with respect to  $q^-$ , we get

$$\begin{aligned} q^- &= \frac{M_1^\perp e^{y_1} + M_2^\perp e^{y_2} - \frac{m_N^2 + t}{2P^+} + \frac{m_N^2}{4(P^+)^2} (M_1^\perp e^{-y_1} + M_2^\perp e^{-y_2})}{2} \pm \\ &\quad + \frac{1}{2} \sqrt{\left(M_1^\perp e^{y_1} + M_2^\perp e^{y_2} - \frac{m_N^2 + t}{2P^+} + \frac{m_N^2}{4(P^+)^2} (M_1^\perp e^{-y_1} + M_2^\perp e^{-y_2})\right)^2 + \frac{Q^2 m_N^2}{(P^+)^2}}, \end{aligned} \quad (11)$$

which allows to express the energy of the photon  $E_\gamma \approx q^-/2$  in terms of the kinematic variables  $(y_a, \mathbf{p}_a^\perp)$  of the produced quarkonia. For asymptotically large energies  $q^-, P^+ \gg \{Q, M_a, m_N, \sqrt{|t|}\}$ , the result (11) reduces to

$$q^- \approx M_1^\perp e^{y_1} + M_2^\perp e^{y_2} \quad (12)$$

and in this limit the variable  $t$  merely reduces to

$$t \approx -(\mathbf{p}_1^\perp + \mathbf{p}_2^\perp)^2. \quad (13)$$

In the photoproduction regime, the expression for  $q^-$  simplifies to

$$q^- = M_1^\perp e^{y_1} + M_2^\perp e^{y_2} - \frac{m_N^2 + t}{2P^+} + \frac{m_N^2}{4(P^+)^2} (M_1^\perp e^{-y_1} + M_2^\perp e^{-y_2}) \quad (14)$$

The invariant energy  $W$  of the  $\gamma p$  collision and the invariant mass  $M_{12}$  of the produced heavy quarkonia pair in terms of these variables might be rewritten as

$$W^2 \equiv s_{\gamma p} = (q + P)^2 = -Q^2 + m_N^2 + 2q \cdot P, \quad (15)$$

and

$$M_{12}^2 = (p_1 + p_2)^2 = M_1^2 + M_2^2 + 2(M_1^\perp M_2^\perp \cosh \Delta y - \mathbf{p}_1^\perp \cdot \mathbf{p}_2^\perp) = \quad (16)$$

$$\begin{aligned} &= t - Q^2 + 2M_1^\perp Q \cosh(y_1 + \delta y_q) + 2M_2^\perp Q \cosh(y_2 + \delta y_q), \\ &\delta y_q = \ln(Q/q^+). \end{aligned} \quad (17)$$

respectively. Finally, the Bjorken variable  $x_B$  might be evaluated using the relation

$$x_B \approx \frac{Q^2 + M_{12}^2}{Q^2 + W_{\gamma p}^2 - m_N^2} \approx \frac{Q^2}{2q^- P^+} + \frac{M_{1\perp}}{P^+} e^{-y_1} + \frac{M_{2\perp}}{P^+} e^{-y_2} \quad (18)$$

The cross-section of electroproduction is dominated by single-photon exchange between leptonic and hadronic parts, and for this reason might be represented as

$$\frac{d\sigma_{ep \rightarrow eM_1 M_2 p}}{d \ln x_B dQ^2 d\Omega_h} = \frac{\alpha_{em}}{\pi Q^2} \left[ (1-y) \frac{d\sigma_{\gamma p \rightarrow M_1 M_2 p}^{(L)}}{d\Omega_h} + \left(1-y + \frac{y^2}{2}\right) \frac{d\sigma_{\gamma p \rightarrow M_1 M_2 p}^{(T)}}{d\Omega_h} \right], \quad (19)$$

where  $y$  is the inelasticity (fraction of electron energy which passes to the virtual photon, which should not be confused with the rapidities  $y_1, y_2$  of produced quarkonia);  $d\Omega_h$  represents the phase volume of the produced quarkonia pair and will be specified below. In (19) we assumed that the incident protons and electrons are not polarized, and  $d\sigma^{(T)}, d\sigma^{(L)}$  are the contributions of the transversely and longitudinally polarized virtual photons. While the former is expected to dominate for longitudinal photons, the latter might get pronounced contributions at large virtualities.

The photoproduction cross-section is related to the amplitude via

$$d\sigma_{\gamma p \rightarrow M_1 M_2 p}^{(L,T)} = \frac{dy_1 dp_{1\perp}^2 dy_2 dp_{2\perp}^2 d\phi_{12} \left| \mathcal{A}_{\gamma p \rightarrow M_1 M_2 p}^{(L,T)} \right|^2}{4(2\pi)^4 \sqrt{(W^2 + Q^2 - m_N^2)^2 + 4Q^2 m_N^2}} \delta\left((q + P_1 - p_1 - p_2)^2 - m_N^2\right) \quad (20)$$

where the  $\delta$ -function guarantees onshellness of the recoil proton. Taking into account that the vectors  $q, P_1$  do not have transverse momenta, we may rewrite the argument of  $\delta$ -function as

$$\begin{aligned} (q + P_1 - p_1 - p_2)^2 - m_N^2 &= \left(q + P_1 - p_1^\parallel - p_2^\parallel\right)^2 - \left(\mathbf{p}_1^\perp + \mathbf{p}_2^\perp\right)^2 - m_N^2 \\ &= \left(q + P_1 - p_1^\parallel - p_2^\parallel\right)^2 - \left((p_1^\perp)^2 + (p_2^\perp)^2 + 2p_1^\perp p_2^\perp \cos \phi_{12}\right) - m_N^2 \end{aligned} \quad (21)$$

where  $\phi_{12}$  is the azimuthal angle between the transverse momenta of quarkonia  $\mathbf{p}_1^\perp, \mathbf{p}_2^\perp$ . We may rewrite the  $\delta$ -function in (21) as

$$\delta\left((q + P_1 - p_1 - p_2)^2 - m_N^2\right) = \frac{\delta(\phi_{12} - \phi_0)}{2p_{1\perp} p_{2\perp} |\sin \phi_0|}, \quad (22)$$

$$\phi_0 = \arccos \left[ \frac{\left(q + P_1 - p_1^\parallel - p_2^\parallel\right)^2 - \left((p_1^\perp)^2 + (p_2^\perp)^2 + m_N^2\right)}{2p_1^\perp p_2^\perp} \right], \quad (23)$$

which allows to integrate out the dependence on  $\phi_{12}$ . The restriction  $|\cos \phi_0| \leq 1$  imposes an additional constraint on possible  $(y_1, p_{1\perp})$  and  $(y_2, p_{2\perp})$  values, at fixed photon-proton energy. In Figure (1) we illustrate the typical kinematically allowed region for a fixed choice of  $E_\gamma, E_p$ , in EIC kinematics, as a function of rapidities and transverse momenta of quarkonia. At very high energies  $P^+, q^- \gg M_{1,2}$ , the domain turns into a narrow strip surrounding the curve (10) and has a typical width  $\sim 1/P^+$ . In this regime the longitudinal momentum of the projectile remains almost constant, so it corresponds to the kinematics  $x_B \sim \xi \ll 1$ , which is outside the scope of our study. The color of each point in Figure (1) illustrates the value of the invariant mass  $M_{12}$  of the quarkonia pair. As we will show below, the dominant contribution to the cross-section comes from the region  $|t|_{\min} \lesssim |t| \lesssim 1 \text{ GeV}^2$ , for this reason we have also shown the line  $t = -1 \text{ GeV}^2$  (the line  $t = t_{\min}$  corresponds to the upper border of each colored domain). The observed anticorrelation between  $|t|$  and  $M_{12}$  might be understood, if we take into account that for fixed-energy of the quarkonia pairs, the variable  $|t|$  reaches its minimum (and  $M_{12}$  reaches its maximum) for quarkonia moving in *opposite* directions; vice versa, quarkonia moving in the *same* direction, will minimize  $M_{12}$  but maximize  $|t|$ . In the experiment, due to finite resolution in the measurement of the photon energy  $W$  and the quarkonia kinematics  $(y_{1,2}, p_{1,2})$ , the narrow domains shown in Figure 1 will get smeared. Due to this, the values of  $M_{12}^2$  and  $t$  are not uniquely defined, but rather are distributed in some interval. The size of this effect depends crucially on the experimental setup, so we won't discuss it here with more detail. However, for any reasonably narrow bins in rapidity ( $\Delta y$ ) or transverse momenta ( $\Delta p_\perp$ ), the variables  $y_{1,2}, p_{1,2}$  remain restricted to some finite domain.

In electroproduction experiments, instead of conventional fixing the photon energy, it might be easier to treat the quarkonia variables  $(y_1, p_{1\perp}, y_2, p_{2\perp}, \phi)$  as independent variables, and express the photon energy in terms of these

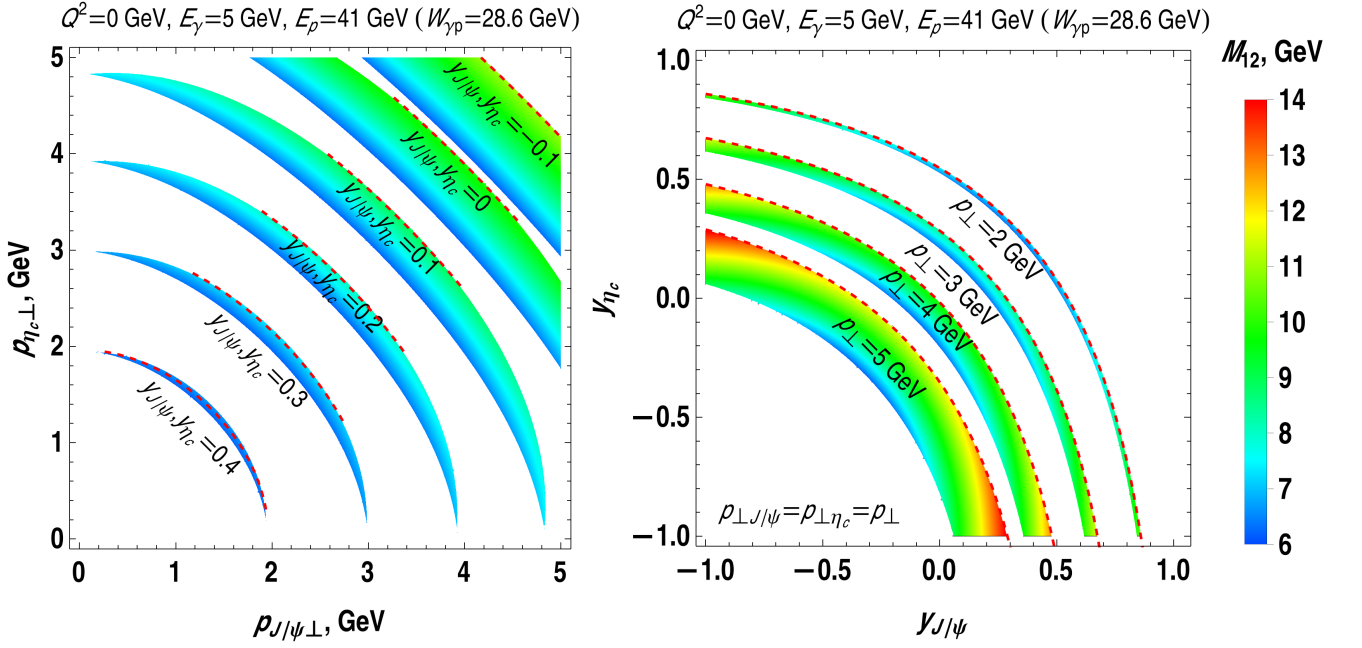


Figure 1. (Color online) The colored bands represent kinematically allowed regions for quarkonia pair production at fixed photon energy  $E_\gamma$ , virtuality  $Q$  and proton energy  $E_p$ . The left plot illustrates the allowed values of transverse momenta for different fixed rapidities  $y_{1,2} \equiv y_{J/\psi}, y_{\eta_c}$  of both quarkonia. An increase of rapidities of both quarkonia leads to higher longitudinal components of their momenta, and thus in view of energy conservation leads to smaller transverse momenta of quarkonia. The right plot illustrates the allowed values of rapidities at different fixed transverse momenta  $|\mathbf{p}_{1,2}| \equiv p_{J/\psi}, p_{\eta_c}$ . Akin to the previous panel, in view of energy conservation, bands with smaller  $p_\perp$  require larger longitudinal components of both quarkonia, which translates into higher quarkonia rapidities. In both plots the color of each point encodes the value of the invariant mass  $M_{12}$  of the quarkonia pair, as given in the color bar legend in the right panel. The red dashed line inside each band corresponds to fixed momentum transfer to the proton  $t = \Delta^2 = -1 \text{ GeV}^2$  (see the text for more explanation).

variables. The  $\delta$ -function in (20) can be rewritten as

$$\begin{aligned} \delta\left((q + P_1 - p_1 - p_2)^2 - m_N^2\right) &= \delta\left(W^2 + M_{12}^2 - 2(q + P_1) \cdot (p_1 + p_2) - m_N^2\right) = \\ &= \frac{\delta(W - W_0) + \delta(W + W_0)}{2W_0}, \end{aligned} \quad (24)$$

$$\begin{aligned} W_0^2 &= 2(q + P_1) \cdot (p_1 + p_2) + m_N^2 - M_{12}^2 = \\ &= \left(q^- + \frac{m_N^2}{2P^+}\right) \cdot (M_1^+ e^{-y_1} + M_2^+ e^{-y_2}) + 2\left(P^+ - \frac{Q^2}{2q^-}\right) \cdot (M_1^+ e^{y_1} + M_2^+ e^{y_2}) + m_N^2 - M_{12}^2. \end{aligned} \quad (25)$$

and  $q^-$  can be fixed from (11). After integration over all possible energies  $W$  (equivalent to integration over all possible  $x_B$ ), we get for the electroproduction cross-section

$$\frac{d\sigma_{ep \rightarrow eM_1 M_2 p}}{dQ^2 d\Omega_h} = \frac{\alpha_{\text{em}}}{4\pi Q^2} \left[ (1-y) \frac{d\bar{\sigma}_{\gamma p \rightarrow M_1 M_2 p}^{(L)}}{d\Omega_h} + \left(1-y + \frac{y^2}{2}\right) \frac{d\bar{\sigma}_{\gamma p \rightarrow M_1 M_2 p}^{(T)}}{d\Omega_h} \right], \quad (26)$$

$$d\bar{\sigma}_{\gamma p \rightarrow M_1 M_2 p}^{(L,T)} = \frac{dy_1 dp_{1\perp}^2 dy_2 dp_{2\perp}^2 d\phi_{12} \left| \mathcal{A}_{\gamma p \rightarrow M_1 M_2 p}^{(L,T)} \right|^2}{4(2\pi)^4 W_0^2 \sqrt{(W_0^2 + Q^2 - m_N^2)^2 + 4Q^2 m_N^2}} \quad (27)$$

where now  $(y_1, p_{1\perp}, y_2, p_{2\perp}, \phi)$  are independent variables, and  $d\bar{\sigma}_{\gamma p \rightarrow M_1 M_2 p}^{(L,T)}$  corresponds to the photoproduction cross-section with photon's energy evaluated using (10).

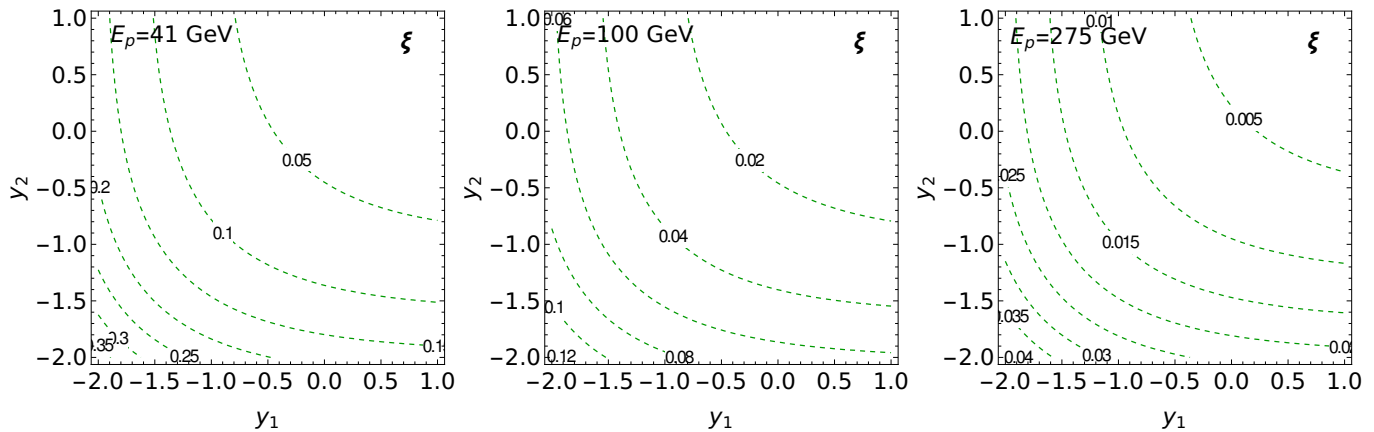


Figure 2. The contour plot illustrates the relation of the skewedness variable  $\xi = -(P_f^+ - P_i^+) / (P_f^+ + P_i^+)$  to the rest-frame quarkonia rapidities  $y_1, y_2$ , for different proton energies  $E_p$ , in EIC kinematics. For the sake of simplicity we consider  $J/\psi \eta_c$  production in the kinematics with zero transverse momenta and zero photon virtuality  $Q$ , which gives the dominant contribution to the total cross-section. Labels on contour lines stand for the values of  $\xi$ .

### B. Amplitudes of the meson pair production process

For the evaluation of the amplitudes  $\mathcal{A}_{\gamma p \rightarrow M_1 M_2 p}^{(a)}$  we will use the collinear factorization framework, which allows to express the amplitude in terms of the target GPDs [1-6]. We will assume that both the photon virtuality  $Q^2$  and the quark mass  $m_Q$  are large parameters, and also disregard the transverse momenta  $\Delta_\perp, \mathbf{p}_{a\perp}$  in the coefficient function. Furthermore, we will assume that the quarkonia pairs are always produced with sufficiently large relative momentum

$$p_{\text{rel}} \approx \frac{(2m_Q) v_{\text{rel}}}{\sqrt{1 - v_{\text{rel}}^2}} \gtrsim \alpha_s (m_Q) m_Q, \quad v_{\text{rel}} = \sqrt{1 - \frac{p_1^2 p_2^2}{(p_1 \cdot p_2)^2}} = \sqrt{1 - \frac{4M_1^2 M_2^2}{(M_{12}^2 - M_1^2 - M_2^2)^2}} \quad (28)$$

both with respect to each other, as well as with respect to recoil proton, to avoid potential factorization breaking by the exchange of soft gluons in the final state. We expect that the factorization should remain valid both in the Bjorken and in the photoproduction regimes.

The GPDs are conventionally defined in the symmetric frame specified in Appendix A, so for the coefficient functions evaluation we will temporarily switch to that frame<sup>2</sup>. In this frame the momenta of the active parton (gluon), before and after interaction, are given explicitly by

$$k_i = \left( (x + \xi) \bar{P}^+, 0, -\frac{\Delta_\perp}{2} \right), \quad k_f = \left( (x - \xi) \bar{P}^+, 0, \frac{\Delta_\perp}{2} \right) \quad (29)$$

where  $x$  is the light-cone fraction of average momentum,  $x = (k_i^+ + k_f^+) / 2\bar{P}^+$ , and the skewedness variable  $\xi$  is related to  $x_B$  defined in (18) via the relations [3]

$$\xi = -\frac{\Delta^+}{2\bar{P}^+} = \frac{x_B}{2 - x_B}, \quad x_B = \frac{2\xi}{1 + \xi}. \quad (30)$$

In exclusive photoproduction, due to relation (18) it is possible to express  $\xi$  in terms of the produced quarkonia momenta. In Figure 2 we illustrate the relation of the variable  $\xi$  to the rapidities  $y_1, y_2$  of the quarkonia in the lab frame.

In Bjorken kinematics, the leading order contribution to the amplitudes of quarkonia production comes from the gluon GPDs. The contributions of the light quark GPDs appear only via higher order loop corrections and

<sup>2</sup> We need to mention that in early studies [2, 3, 69, 70], the GPDs were defined in an asymmetric frame, in which the momentum transfer of the incident photon is zero. Up to a trivial longitudinal boost this frame essentially coincides with the frame introduced in Section II A. It is possible to relate the GPDs defined in different frames using some transformation of the arguments. However, since this frame is not widely used in the recent literature dedicated to GPD properties, we abstain from using it in what follows.

thus will be omitted in what follows. Furthermore, we will disregard the contributions of the transversity gluon GPDs  $H_T^g$ ,  $E_T^g$ ,  $\tilde{H}_T^g$ ,  $\tilde{E}_T^g$ , since at present there is no phenomenological parametrizations for these GPDs, and existing experimental bounds suggest that they should be negligibly small (see e.g. explanation in [81, 88]). By their definition, the transversity GPDs appear in the amplitudes multiplied by the momentum transfer to the proton  $\Delta$ , which is small in the kinematics of interest, so we expect that their omission should be numerically justified. The contribution of the chiral even GPDs to the square of amplitude is given by

$$\sum_{\text{spins}} \left| \mathcal{A}_{\gamma p \rightarrow M_1 M_2 p}^{(\mathbf{a})} \right|^2 = \frac{1}{(2-x_B)^2} \left[ 4(1-x_B) \left( \mathcal{H}_{\mathbf{a}} \mathcal{H}_{\mathbf{a}}^* + \tilde{\mathcal{H}}_{\mathbf{a}} \tilde{\mathcal{H}}_{\mathbf{a}}^* \right) - x_B^2 \left( \mathcal{E}_{\mathbf{a}} \mathcal{E}_{\mathbf{a}}^* + \mathcal{E}_{\mathbf{a}} \mathcal{H}_{\mathbf{a}}^* + \tilde{\mathcal{H}}_{\mathbf{a}} \tilde{\mathcal{E}}_{\mathbf{a}}^* + \tilde{\mathcal{E}}_{\mathbf{a}} \tilde{\mathcal{H}}_{\mathbf{a}}^* \right) \right. \\ \left. - \left( x_B^2 + (2-x_B)^2 \frac{t}{4m_N^2} \right) \mathcal{E}_{\mathbf{a}} \mathcal{E}_{\mathbf{a}}^* - x_B^2 \frac{t}{4m_N^2} \tilde{\mathcal{E}}_{\mathbf{a}} \tilde{\mathcal{E}}_{\mathbf{a}}^* \right], \quad \mathbf{a} = L, T \quad (31)$$

where the index  $\mathbf{a}$  refers to longitudinal or transverse photons, and, inspired by similar analysis of Compton scattering and single-meson deeply virtual production [74, 75], we introduced the double meson form factors

$$\mathcal{H}_{\mathbf{a}}(y_1, y_2, t) = \int dx c_{\mathbf{a}}(x, y_1, y_2) H_g(x, \xi, t), \quad \mathcal{E}_{\mathbf{a}}(y_1, y_2, t) = \int dx c_{\mathbf{a}}(x, y_1, y_2) E_g(x, \xi, t), \quad (32)$$

$$\tilde{\mathcal{H}}_{\mathbf{a}}(y_1, y_2, t) = \int dx \tilde{c}_{\mathbf{a}}(x, y_1, y_2) \tilde{H}_g(x, \xi, t), \quad \tilde{\mathcal{E}}_{\mathbf{a}}(y_1, y_2, t) = \int dx \tilde{c}_{\mathbf{a}}(x, y_1, y_2) \tilde{E}_g(x, \xi, t), \quad (33)$$

where the variable  $\xi$  should be understood as a function of  $y_1, y_2$ , as defined in (30). The corresponding partonic amplitudes  $c_{\mathbf{a}}, \tilde{c}_{\mathbf{a}}$  might be evaluated perturbatively, taking into account the diagrams shown in the Figures 3, 4. Since we assume that produced quarkonia are well-separated from each other kinematically, the final Fock state of the system is a direct product of Fock states of individual quarkonia, and thus it is possible to express the amplitudes  $c_{\mathbf{a}}, \tilde{c}_{\mathbf{a}}$  in terms of the wave functions or distribution amplitudes which encode the nonperturbative structure of individual quarkonia. According to NRQCD and potential models, the dominant Fock state in charmonium is the color singlet  $\bar{c}c$  pair in  $^3S_1^{[1]}$  state for  $J/\psi$ , and  $^1S_0^{[1]}$  state for  $\eta_c$ . The distribution of the quarks over the light-cone momenta might be described by the corresponding distribution amplitudes  $\Phi_M(z_a)$ , where  $z_a$  is the fraction of the quarkonium light-cone momentum carried by the quark. The relative velocity of heavy quarks inside the quarkonia in the heavy quark mass limit is suppressed as  $\sim \alpha_s(m_Q) \ll 1$ , and for this reason both heavy quarks inside each quarkonia carry approximately half of its momentum. In this approximation, we may replace both distribution amplitudes  $\Phi_{\eta}, \Phi_{J/\psi}$  with

$$\Phi_{J/\psi}(z) \approx f_{J/\psi} \delta(z-1/2), \quad \Phi_{\eta_c}(z) \approx f_{\eta_c} \delta(z-1/2), \quad (34)$$

where  $f_{J/\psi}, f_{\eta_c}$  are the (nonperturbative) decay constants of the corresponding quarkonia states. In the language of NRQCD,  $f_{J/\psi}^2$  and  $f_{\eta_c}^2$  are proportional to the color singlet Long Distance Matrix Elements (LDMEs)  $\langle \mathcal{O}_{J/\psi}^{[1]} \left( ^3S_1^{[a]} \right) \rangle$ ,  $\langle \mathcal{O}_{\eta_c}^{[1]} \left( ^1S_0^{[a]} \right) \rangle$  respectively [34, 56]. In this approach, the functions  $c_{\mathbf{a}}, \tilde{c}_{\mathbf{a}}$  might be related to partonic-level amplitudes  $C_{\mathbf{a}}, \tilde{C}_{\mathbf{a}}$  as

$$c_{\mathbf{a}}(x, y_1, y_2) = \int dz_1 dz_2 C_{\mathbf{a}}(x, z_1, z_2, y_1, y_2) \Phi_{\eta}(z_1) \Phi_{J/\psi}(z_2) \approx f_{J/\psi} f_{\eta_c} C_{\mathbf{a}} \left( x, \frac{1}{2}, \frac{1}{2}, y_1, y_2 \right) + \mathcal{O}(\alpha_s(m_c)) \quad (35)$$

$$\tilde{c}_{\mathbf{a}}(x, y_1, y_2) = \int dz_1 dz_2 \tilde{C}_{\mathbf{a}}(x, z_1, z_2, y_1, y_2) \Phi_{\eta}(z_1) \Phi_{J/\psi}(z_2) \approx f_{J/\psi} f_{\eta_c} \tilde{C}_{\mathbf{a}} \left( x, \frac{1}{2}, \frac{1}{2}, y_1, y_2 \right) + \mathcal{O}(\alpha_s(m_c)), \quad (36)$$

and  $C_{\mathbf{a}}, \tilde{C}_{\mathbf{a}}$  might be evaluated in perturbative QCD. Assuming equal sharing of quarkonium momentum between constituent quarks, it is possible to show that the typical virtuality of the gluon connecting different heavy lines is parametrically of order  $\sim M_{12}^2/4$  for the diagrams in Figures 3, and of order  $\sim \min(M_1^2, M_2^2)$  for the diagrams in Figure 4. This justifies the applicability of perturbation theory for evaluation of  $C_{\mathbf{a}}, \tilde{C}_{\mathbf{a}}$ , even for the diagrams which include 3-gluon vertices in Figure 3. The full expressions for the amplitudes are provided in Appendix B.

The contribution of longitudinal photons to  $C_{\mathbf{a}}$  vanishes in the limit of small  $\mathbf{p}_{a\perp} \ll M, Q$  in view of combined Lorentz- and  $P$ -parity. The contributions of the longitudinal photons to  $\tilde{C}_{\mathbf{a}}$  do not vanish in this limit, although in the cross-section it appears in convolution with numerically small helicity flip gluon GPDs  $\tilde{H}_g, \tilde{E}_g$ . Since for quasireal photons the contribution of longitudinal photons is suppressed by a factor  $Q/m_Q$ , we will disregard it altogether in the total (unpolarized) cross-section.

The dependence on the variable  $x$  in the coefficient functions might be represented as a linear superposition of rational expressions

$$C_a \left( x, \frac{1}{2}, \frac{1}{2}, y_1, y_2 \right) \sim \sum_{\ell} \frac{\mathcal{P}_{\ell}(x)}{\prod_{k=1}^{n_{\ell}} (x - x_k^{(\ell)} + i0)} \quad (37)$$

where  $\mathcal{P}_{\ell}(x)$  is a smooth polynomial of the variable  $x$ , and the denominator of each term in the sum (37) might include a polynomial with up to  $n_{\ell} = 5$  nodes  $x_k^{(\ell)}$  in the region of integration. The integral near the poles exists only in the principal value sense and is evaluated using

$$\frac{1}{x - x_k^{(\ell)} + i0} = \text{P.V.} \left( \frac{1}{x - x_k^{(\ell)}} \right) - i\pi \delta(x - x_k^{(\ell)}) \quad (38)$$

The position of the poles  $x_k^{(\ell)}$  depends on all kinematic variables  $y_1, y_2, Q$ . In Figure 5 we show the density plot which illustrates the behavior of the coefficient function  $C_T(x, \xi, z_1 = z_2 = 1/2, y_1, y_2)$  as a function of its arguments. While in the convolution integrals (32-33) we need to take integral over all  $x \in (-1, 1)$ , we expect that a sizable contribution comes from the region near the poles of the coefficient function. From the Figure 5 we can see that in the coefficient function there are several poles, whose location depends on the kinematics of produced quarkonia. For the special case  $Q = 0$  and  $y_1 = y_2$  it is possible to express the position of these poles in terms of the variable  $\xi$  as

$$|x_k| = \left\{ \xi, \xi \left( 1 - \frac{1}{1+\xi} \right), \xi \left( 1 - \frac{1}{2} \frac{1}{1+\xi} \right), \xi \left( 1 - \frac{2}{3} \frac{1}{1+\xi} \right), \xi \left( 1 - \frac{1}{3} \frac{1}{1+\xi} \right), 3\xi \left( 1 + \frac{1}{6} \frac{1}{1+\xi} \right) \right\}. \quad (39)$$

Varying the rapidities  $y_1, y_2$  of the observed quarkonia and virtuality  $Q^2$  of the photon, it is possible to probe the gluon GPDs in the full kinematic range  $(x, \xi)$ . For this reason, the information about the gluon GPDs extracted from this process is complementary to what could be extracted from single quarkonia production or DVCS, which are mostly sensitive to gluon GPD near  $x \approx \pm \xi$ .

According to NRQCD [22–33], the color octet  $\bar{Q}Q$  states might also contribute to quarkonia production, so the expression (31) should be generalized as

$$\sum_{\text{spins}} \left| \mathcal{A}_{\gamma p \rightarrow J/\psi \eta_c p}^{(a)} \right|^2 \approx \sum_{ij} \langle \mathcal{O}_i^{(J/\psi)} \rangle \langle \mathcal{O}_j^{(\eta_c)} \rangle \left| \mathcal{A}_{\gamma TP \rightarrow [\bar{Q}Q]_i [\bar{Q}Q]_j p} \right|^2, \quad (40)$$

where  $\langle \mathcal{O}_i^{(M)} \rangle$  are the nonperturbative color singlet and octet Long Distance Matrix Elements (LDMEs) corresponding to a given state  $i$  of the  $\bar{Q}Q$ . In the heavy quark mass limit, the series (40) is expected to converge rapidly, so for numerical evaluations usually only the first few terms are relevant. As mentioned earlier, the dominant color singlet contribution is controlled by the LDMEs  $\langle \mathcal{O}_{J/\psi} \left( {}^3S_1^{[a]} \right) \rangle$ ,  $\langle \mathcal{O}_{\eta_c} \left( {}^1S_0^{[a]} \right) \rangle$ , which according to phenomenological estimates have comparable values [84]

$$\langle \mathcal{O}_{J/\psi} \left( {}^3S_1^{[a]} \right) \rangle \approx \langle \mathcal{O}_{\eta_c} \left( {}^1S_0^{[a]} \right) \rangle \approx 0.3 \text{ GeV}^3. \quad (41)$$

The evaluation of the color octet amplitudes  $\mathcal{A}_{\gamma TP \rightarrow [\bar{Q}Q]_s [\bar{Q}Q]_s p}$  is very similar to the color singlet case and differs only due to different choice of the spin-color projections. However, according to phenomenological estimates, the color octet LDMEs of  $J/\psi$  mesons are very small [32],

$$\langle \mathcal{O}^{J/\psi} \left( {}^3S_1^{[8]} \right) \rangle \approx 2.32 \times 10^{-4} \text{ GeV}^3, \quad (42)$$

$$\langle \mathcal{O}^{J/\psi} \left( {}^1S_0^{[8]} \right) \rangle \approx 8.35 \times 10^{-3} \text{ GeV}^3, \quad (43)$$

$$\langle \mathcal{O}^{J/\psi} \left( {}^3P_0^{[8]} \right) \rangle \approx 0, \quad (44)$$

and the color octet LDMEs of the  $\eta_c$  should be of the same order in view of the heavy quark mass limit relations [22]

$$\langle \mathcal{O}^{\eta_c} \left( {}^1S_0^{[a]} \right) \rangle = \frac{1}{3} \langle \mathcal{O}^{J/\psi} \left( {}^3S_1^{[a]} \right) \rangle, \quad a = 1, 8, \quad (45)$$

$$\langle \mathcal{O}^{\eta_c} \left( {}^3S_1^{[8]} \right) \rangle = \langle \mathcal{O}^{J/\psi} \left( {}^1S_0^{[8]} \right) \rangle, \quad (46)$$

$$\langle \mathcal{O}^{\eta_c} \left( {}^1P_1^{[8]} \right) \rangle = 3 \langle \mathcal{O}^{J/\psi} \left( {}^3P_0^{[8]} \right) \rangle. \quad (47)$$



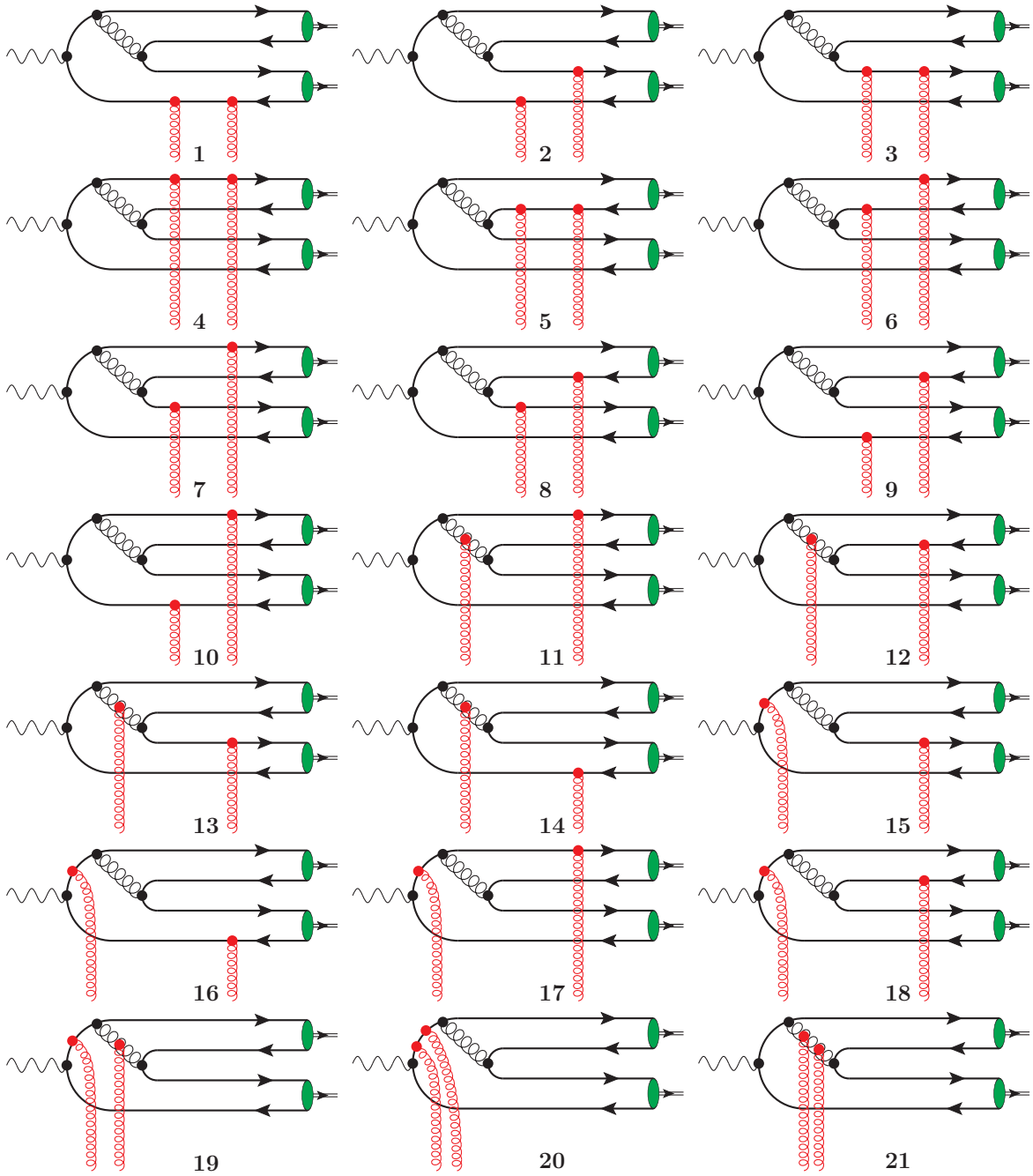


Figure 3. Schematic illustration of the single quark loop (“type- $A$ ”) diagrams which contribute to the meson pair production. In all plots it is implied inclusion of diagrams which might be obtained by inversion of heavy quark lines (“charge conjugation”).

For this reason, in what follows we may safely omit the color octet contributions<sup>3</sup>.

<sup>3</sup> We need to mention that at very large transverse momenta  $p_T \gtrsim 5-10$  GeV it is known that color octet contributions might give relevant contribution to inclusive quarkonia production [27, 28, 34]. However, in our evaluations we do not consider such large values of  $p_T$ , since the exclusive cross-section is strongly suppressed in that kinematics due to suppression of gluon GPDs at large  $|t| \sim p_{\perp}^2$ .

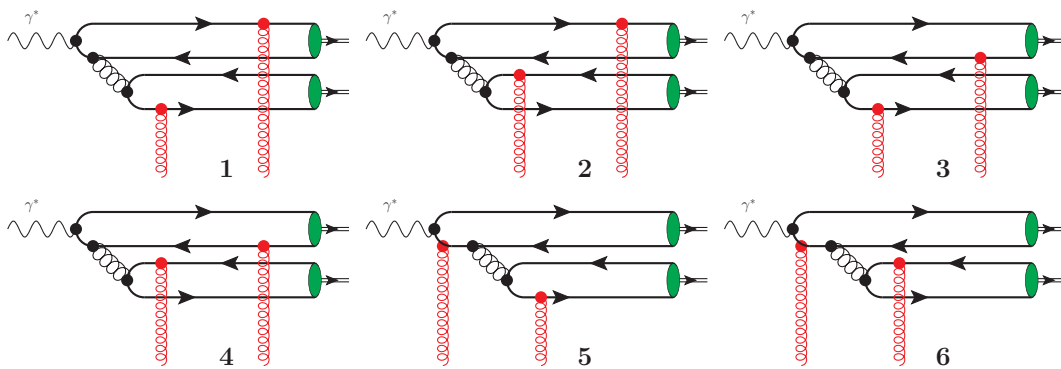


Figure 4. Schematic illustration of the double quark loop (“type-B”) diagrams which contribute to the meson pair production. In all plots it is implied inclusion of diagrams which might be obtained by inversion of heavy quark lines (“charge conjugation”) in the first loop; diagrams 2,4,6 are related to diagrams 1,3,5 by charge conjugation (symmetry  $z_2 \rightarrow 1 - z_2$ ).

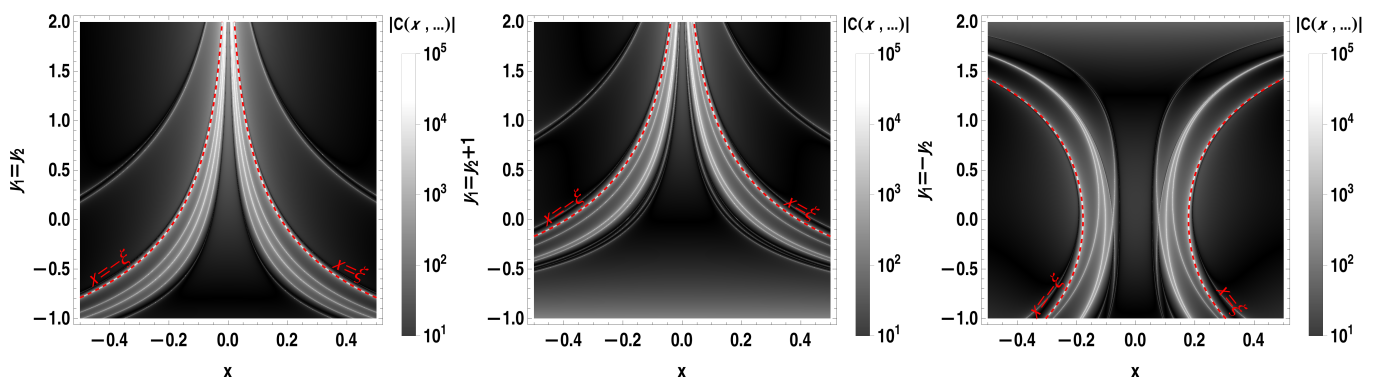


Figure 5. Density plot which illustrates the coefficient function  $C_T$  (in relative units) as a function of the variables  $x$  and quarkonia rapidities  $y_1, y_2$ . Left, central and right plots correspond to  $y_1 = y_2$ ,  $y_1 = y_2 + 1$  and  $y_1 = -y_2$  respectively. Rapidities are taken in the lab frame, for proton energy  $E_p^{(1)} = 41$  GeV; for other proton energies rapidities should be shifted by  $\Delta y = \ln(E_p/E_p^{(1)})$ . For the sake of definiteness, we considered the photoproduction regime ( $Q = 0$ ) in all plots. White lines effectively demonstrate the position of the poles  $x_k^\ell$  of the coefficient function (37). For reference, we marked with red dashed lines the poles which correspond to  $x = \pm\xi$ , where the skewedness  $\xi = \xi(y_1, y_2)$  was evaluated using (18,30).

### III. NUMERICAL RESULTS

For the sake of definiteness, for our predictions we use the Kroll-Goloskokov parametrization of the gluon GPDs [76–81]. This parametrization effectively takes into account the evolution of the gluon distributions, introducing a mild dependence of the model parameters on the factorization scale  $\mu_F$ . In what follows for the sake of definiteness we will choose the scale  $\mu_F = \mu_R \approx \sqrt{M_{J/\psi}^2 + Q^2}$ , which interpolates smoothly between  $\mu_F \approx M_{J/\psi}$  in photoproduction regime, and  $\mu_F \approx Q$  in Bjorken regime. In Figure 6 we show the dependence of the typical cross-section on the choice of this factorization scale. We may observe that this dependence is mild at moderate energies, but becomes very pronounced at very high energies (small  $x_B$ ). Such behaviour is not surprising: it is known from studies of *single* quarkonia photoproduction [34–37] that this dependence is due to omitted loop corrections, and these corrections become especially pronounced in the small- $x_B$  kinematics.

We would like to start the presentation of results with a discussion of the cross-section (27) dependence on the virtuality  $Q$ , shown schematically in Figure 7. This dependence is very mild in the photoproduction regime ( $Q \lesssim M_{J/\psi}$ ), since the hard scale in this kinematics is controlled by the quarkonium mass. In Bjorken regime ( $Q \gg M_{J/\psi}$ ) the virtuality  $Q$  plays the role of the hard scale, which leads to a pronounced dependence on  $Q$ . We can see that the cross-section is strongly suppressed, so the experimental studies of this regime become very challenging. For small  $Q \lesssim M_{J/\psi}$ , the cross-section is dominated by the transversely polarized  $J/\psi$  mesons, similar to single  $J/\psi$  production. This contribution is sensitive to the gluon GPDs  $H_g, E_g$ . The contribution of the longitudinally polarized  $J/\psi$  mesons

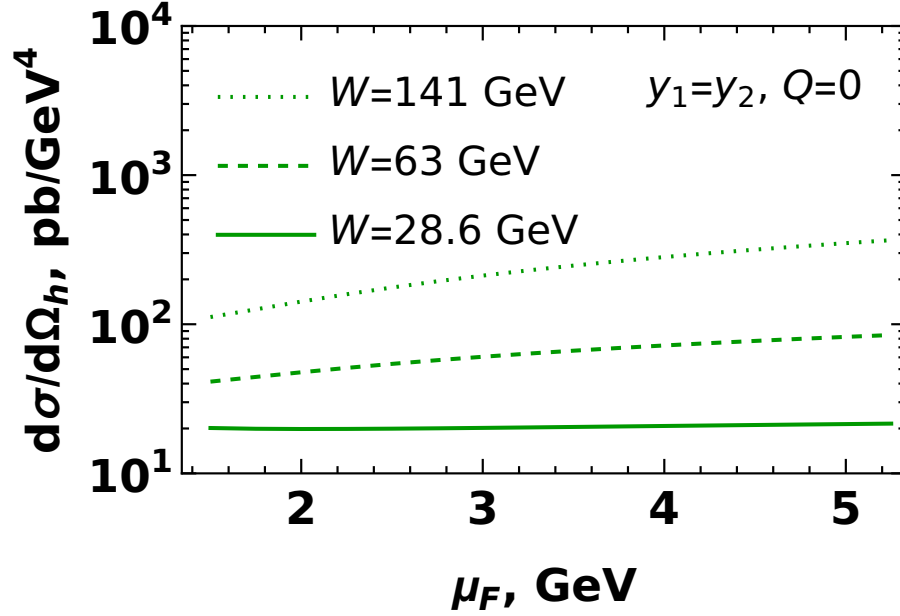


Figure 6. Dependence of the cross-section on the choice of factorization scale  $\mu_F$ . The frame label  $d\sigma/d\Omega_h$  on the vertical axis is a shorthand notation for  $d\sigma/dy_1 dp_1^2 dy_2 dp_2^2 d\phi$ . Chosen values of  $W$  correspond to photon-proton energies  $E_\gamma \times E_p = 18 \times 275$  GeV,  $100 \times 10$  GeV and  $5 \times 41$  GeV respectively. In photoproduction regime these values of  $W$  correspond to values of Bjorken variable  $x_B \approx 1.9 \times 10^{-3}$ ,  $9.4 \times 10^{-3}$  and  $4.5 \times 10^{-2}$  respectively. All frame-dependent variables are given in the laboratory reference frame described in Section II A.

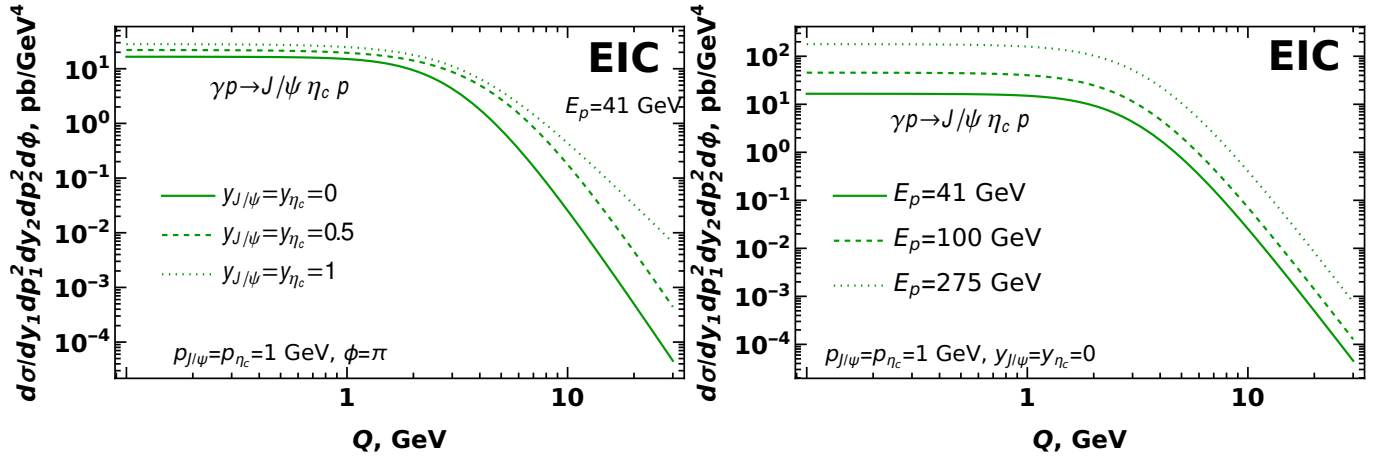


Figure 7. Dependence of the photoproduction cross-section (27) on the virtuality  $Q$  of the photon. In the left and right plots we compare predictions for different rapidities  $y_{J/\psi}, y_{\eta_c}$  and different proton energies  $E_p$ . Both plots clearly illustrates the transition from photoproduction to Bjorken regime in the region  $Q \sim 1 - 2 M_{J/\psi}$ . In both plots the photon energy is evaluated from (1,11). All frame-dependent variables are given in the reference frame described in Section II A.

is controlled by the helicity flip gluon GPDs  $\tilde{H}_g, \tilde{E}_g$ , which are less known phenomenologically, although they are clearly significantly smaller than the unpolarized GPDs. We also observe that the GPDs  $H_g, E_g$  might contribute to longitudinally polarized photons via  $\sim \mathcal{O}(\mathbf{p}_{\perp J/\psi})$  corrections, although a systematic analysis of this contribution would also require to take into account currently unknown twist-3 gluon GPDs. In view of these uncertainties, we abstain from making predictions for the longitudinal polarization.

In Figure 8 we show the dependence of the cross-section (27) on the transverse momenta  $\mathbf{p}_{1\perp}, \mathbf{p}_{2\perp}$ . In the collinear factorization approach this dependence is largely due to the gluon GPD dependence on the invariant momentum transfer  $t$  (8): most of the phenomenological models implement a pronounced (nearly exponential) behavior at small

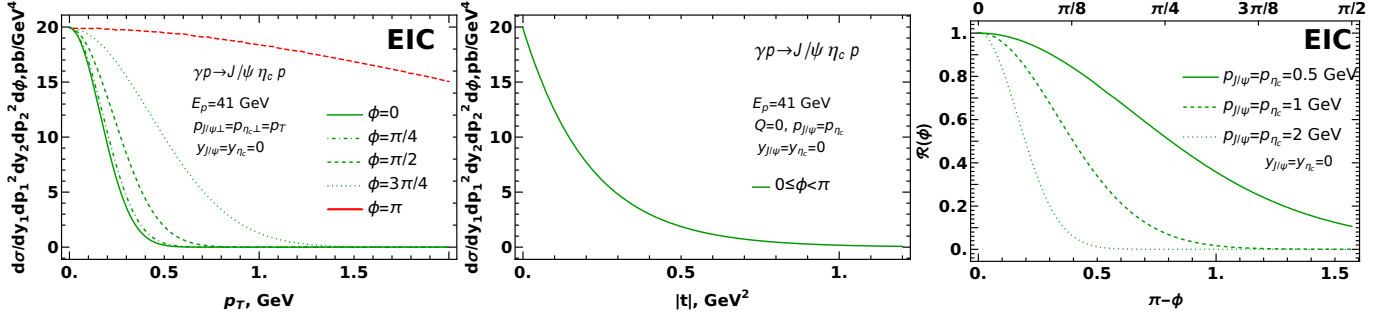


Figure 8. Dependence of the photoproduction cross-section (27) on the transverse momenta  $p_T$  of the quarkonia (left panel), invariant momentum transfer  $t$  to the proton (central panel) and the angle  $\phi$  between the quarkonia (right panel). Since the cross-sections at different  $p_T$  differ quite significantly, in order to facilitate the comparison of their  $\phi$ -dependence, in the right plot we normalized them to unity in the maximum (angle  $\phi = \pi$ ). For the sake of definiteness, we considered the case photoproduction ( $Q = 0$ ) at central rapidities ( $y_1 = y_2 = 0$ ) in the lab frame; for other virtualities and rapidities the  $p_T$ - and  $\phi$ -dependence have very similar shapes. All frame-dependent variables are given in the reference frame described in Section II A.

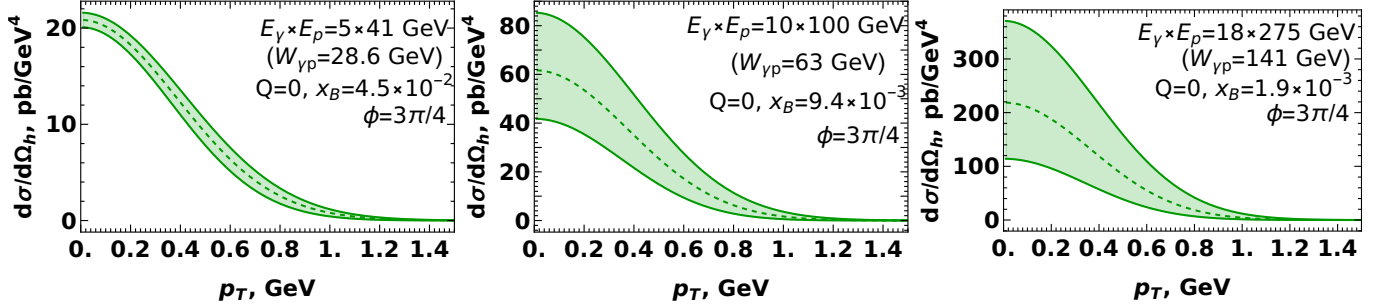


Figure 9. Uncertainty of the cross-section due to choice of factorization scale  $\mu_F$ . In all plots central dashed line corresponds to  $\mu_F = M_{J/\psi}$ , whereas upper and lower limits of the colored bands correspond to  $\mu_F = 2M_{J/\psi}$  and  $\mu_F = M_{J/\psi}/2$  respectively. For the sake of definiteness, in all plots we considered that the angle between  $J/\psi$  and  $\eta_c$  is  $\phi = 3\pi/4$ ; for other angles the uncertainty due to choice of  $\mu_F$  has the same magnitude.

$t$ . At large angles  $\phi \approx \pi$  between transverse momenta of quarkonia (back-to-back kinematics) the cross-section has a sharp peak, which might be understood from the definition (8): this point minimizes  $|t|$  at fixed  $|p_{1\perp}|, |p_{2\perp}|$ . As discussed in Section II A, the transverse momenta  $\mathbf{p}_{1\perp}, \mathbf{p}_{2\perp}$  also appear in other observables (e.g. via kinematic constraints, “transverse” masses  $M_{1,2}^\perp$ ) and thus a mild  $p_T$ -dependence exists even for  $\mathbf{p}_{1\perp} = -\mathbf{p}_{2\perp}$ , as could be seen from the red long-dashed line in the left panel of the Figure 8. Since in the collinear approach we neglected the  $p_T$ -dependence in the coefficient functions, the results are valid only for small  $p_T \ll \max(Q, m_Q)$ ; in the opposite limit (wide angle scattering kinematics) the cross-section will be strongly suppressed as a function of the variable  $p_T$  even for  $p_T = \mathbf{p}_{1\perp} = -\mathbf{p}_{2\perp}$ . The central panel in the Figure 8 clearly demonstrates that for any fixed  $\phi \neq \pi$ , the cross-section has the same dependence on invariant momentum transfer  $t$ . This happens because in collinear approach we disregard the transverse momenta in evaluation of the coefficient function, so  $\phi$ -dependence exists only due to  $t$ -dependence of the gluon GPDs. In the Figure 9 we illustrate the uncertainty of these cross-sections due to choice of the scale  $\mu_F$ , varying it in the range  $\mu_F \in (M_{J/\psi}/2, 2M_{J/\psi})$ . As discussed earlier, this uncertainty is very moderate at low energies, yet becomes very pronounced (up to a factor of two) at high energies. This indicates that loop corrections might give pronounced contribution in that kinematics.

In Figure 10 we show the dependence of the  $p_T$ -integrated cross-section on the rapidities of the produced quarkonia. In the left panel, we show the dependence of the cross-section on the average rapidity  $y_1 = y_2$ . As expected, the cross-section grows with  $y$  due to the increase of photon energy,  $W^2$ , the corresponding decrease of  $x_B, \xi$  and the growth of the gluon GPDs in that kinematics. In the right panel we show the dependence on the rapidity difference  $\Delta y$  at central rapidities. The cross-section decreases as a function of  $\Delta y$ , because the variables  $x_B, \xi$ , the longitudinal recoil to the proton, and the longitudinal momentum transfer  $|t_{\min}|$  grow as a function of  $\Delta y$  at fixed  $Y$ , and the amplitude decreases due to suppression of gluon GPDs with  $|t|$ . Finally, in Figure 11 we show the distribution of the produced  $J/\psi \eta_c$  pairs over their invariant mass  $M_{12}$ . The distribution has a pronounced peak near  $M_{12} \approx 7$  GeV, which demonstrates that the quarkonia pairs predominantly are produced with a small relative momentum  $\sim 2 - 3$

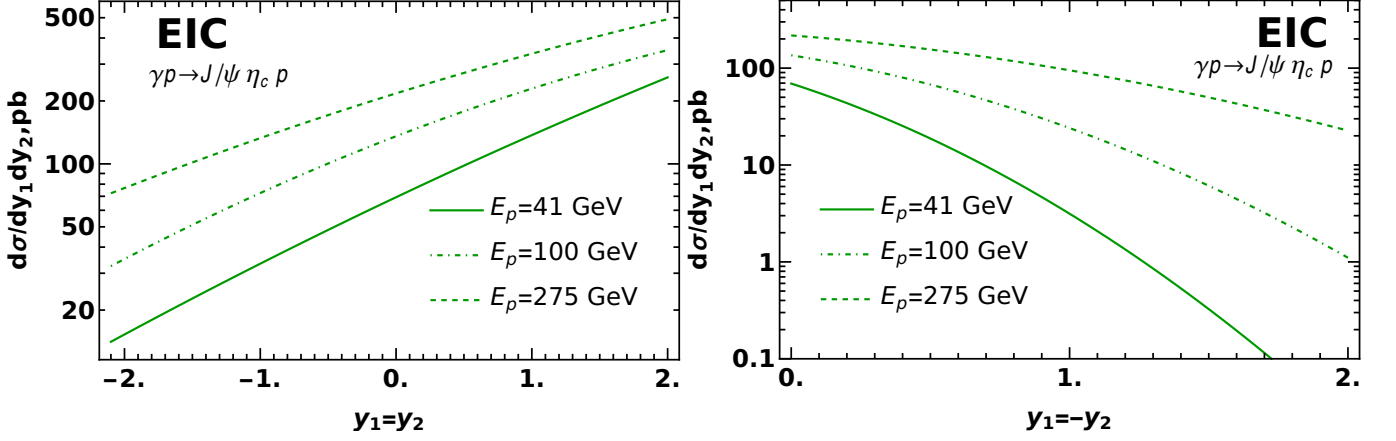


Figure 10. Dependence of the cross-section on the rapidities  $y_1, y_2$  of the two quarkonia for several proton energies in EIC kinematics. In the left plot we illustrate the dependence on the average rapidity ( $y_1 = y_2$ ), and in the right plot we consider the dependence on the rapidity difference at central rapidities ( $y_1 = -y_2 = \Delta y/2$ ).

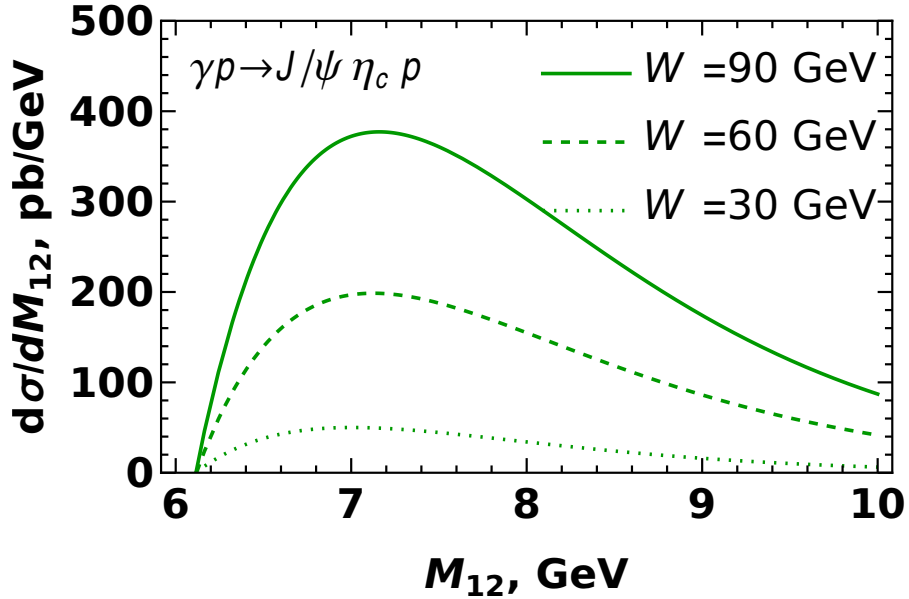


Figure 11. Distribution of the produced quarkonia pairs over their invariant mass  $M_{12}$ , for several fixed invariant energies  $W$  of the  $\gamma p$  collision.

GeV.

#### IV. CONCLUSIONS

In this paper we studied, in the collinear factorization approach, the exclusive photoproduction of heavy charmonia pairs with opposite  $C$ -parities ( $J/\psi \eta_c$ ). In our analysis we focused on the kinematics of moderate values of  $x_B$ , achievable with low-energy  $ep$  beams at the Electron Ion Collider. This regime corresponds to values of Bjorken variable  $x_B \in (10^{-3}, 10^{-1})$ . We performed evaluations in leading order, assuming that higher order corrections are suppressed at least as  $\alpha_s(m_Q)$ . We focused on the photoproduction regime ( $Q^2 \approx 0$ ) and found that the dependence of the photoproduction cross-section on the virtuality  $Q$  is quite mild up to  $Q \lesssim m_Q \approx 1.2 - 1.5$  GeV. The cross-section has a pronounced dependence on the invariant momentum transfer  $t$ , and vanishes for  $|t| \gtrsim 1$  GeV<sup>2</sup>. This implies that the quarkonia pairs are produced predominantly in back-to-back kinematics (with oppositely directed

transverse momenta), which minimizes  $|t|$ . The produced  $J/\psi$  mesons are predominantly transversely polarized, and the amplitude of the process obtains the dominant contribution from the unpolarized gluon GPD  $H_g$ . The coefficient function (partonic amplitude) has several poles (in addition to the classical  $x = \pm\xi$ ), whose positions depend on the kinematics of the produced quarkonia. In view of the complexity of the coefficient function, the deconvolution (direct extraction of GPDs from amplitudes) is apparently not possible. Nevertheless, we believe that the process might be useful to constrain existing models of phenomenological GPDs, especially outside the  $x = \pm\xi$  line.

The results presented here complement our earlier analysis [59] done in the color dipole framework in the kinematics  $x_B \ll 1$ , and agrees with it by an order of magnitude if extended to the region of common validity (largest energy  $ep$  beams at EIC, small  $x_B \ll 1$ ). However, the collinear factorization approach might be not reliable there due to large NLO corrections and onset of saturation effects.

Numerically, the evaluated cross-sections are on par with similar estimates for  $2 \rightarrow 3$  processes ( $\gamma^*p \rightarrow \gamma Mp$ ,  $M = \pi, \rho$ ) suggested recently in the literature [8–17]. This happens because the emission of a photon in the final state leads to a suppression by the fine-structure constant  $\alpha_{\text{em}}$ , on par with the suppression due to heavy quark mass in the production of heavy quarkonia pairs. For this reason both  $\gamma^*p \rightarrow \gamma Mp$  and heavy quarkonia production could be used as complementary tools for the study of both quark and gluon GPDs.

## ACKNOWLEDGEMENTS

We thank our colleagues at UTFSM university for encouraging discussions. This research was partially supported by Proyecto ANID PIA/APOYO AFB180002 (Chile) and Fondecyt (Chile) grants 1180232 and 1220242. "Powered@NLHPC: This research was partially supported by the supercomputing infrastructure of the NLHPC (ECM-02)".

## Appendix A: Symmetric frame

In the collinear factorization framework the evaluations in Bjorken kinematics are frequently performed in the so-called symmetric frame [2, 3, 67, 69–73], in which the vectors of photon momentum  $q$  and  $\bar{P} = (P_i + P_f)/2$  (the average momentum of the target before and after collision) do not have transverse momenta. This frame differs from the lab-frame introduced in Section II A by a transverse boost, supplemented by a rotation in the transverse plane [3]. In this paper we focus on the kinematics of small transverse momenta  $\Delta_\perp$ , which eventually will be disregarded during evaluations of the coefficient functions, so the parameters of the boost and rotation are also small,  $\sim \Delta_\perp/P^+$ , and will give only  $\mathcal{O}(\Delta_\perp^2)$  corrections to  $\pm$  components of light-cone vectors. For this reason, in what follows we will abuse notations and disregard possible differences of  $\pm$  components in lab- and symmetric frames.

Explicitly, the light-cone decomposition of photon and proton momenta is given by

$$q = \left( Z\bar{P}^+, -\frac{Q^2}{2Z\bar{P}^+}, \mathbf{0}_\perp \right), \quad (\text{A1})$$

$$\bar{P} = \frac{P_f + P_i}{2} = \left( \bar{P}^+, \frac{\bar{m}_N^2}{2\bar{P}^+}, \mathbf{0}_\perp \right), \quad \bar{m}_N^2 = m_N^2 - \frac{t}{4} \quad (\text{A2})$$

$$\Delta = P_f - P_i = \left( -2\xi\bar{P}^+, \frac{\xi\bar{m}_N^2}{\bar{P}^+}, \Delta_\perp \right) \quad (\text{A3})$$

so the momenta of proton before collision ( $P_i$ ) and after collision ( $P_f$ ) are given explicitly by

$$P_{f,i} = P \pm \frac{\Delta}{2} = \left( (1 \mp \xi)\bar{P}^+, (1 \pm \xi)\frac{\bar{m}_N^2}{2\bar{P}^+}, \pm \frac{\Delta_\perp}{2} \right) \quad (\text{A4})$$

and the invariant momentum transfer to the proton is

$$t = \Delta^2 = -4\xi^2 \left( m_N^2 - \frac{t}{4} \right) - \Delta_\perp^2 = -\frac{4\xi^2 m_N^2 + \Delta_\perp^2}{1 - \xi^2}. \quad (\text{A5})$$

The variable  $\bar{P}^+$  might be related to variables defined in Section II A as

$$\bar{P}^+ = P^+ + \frac{q^+ - M_1^\perp e^{-y_1} - M_2^\perp e^{-y_2}}{2} = \frac{m_N^2}{2P^-} + \frac{q^+ - M_1^\perp e^{-y_1} - M_2^\perp e^{-y_2}}{2} \quad (\text{A6})$$

The variable  $Z$  might be fixed from conservation of plus-components of momenta as

$$Z = \frac{q^+}{\bar{P}^+} = -2\xi + \frac{M_{1\perp}}{2\bar{P}^+} e^{-y_1} + \frac{M_{2\perp}}{2\bar{P}^+} e^{-y_2}. \quad (\text{A7})$$

### Appendix B: Evaluation of the coefficient functions

The evaluation of the coefficient functions (partonic amplitudes) relies on standard light-cone rules formulated in [1, 3, 39, 67, 82, 83]. We assume that both photon virtuality  $Q$  and the quark mass  $m_Q$  are large parameters,  $Q \sim m_Q \sim \sqrt{s_{\gamma p}}$ , tacitly disregarding the proton mass and momentum transfer to the proton  $t$ . As we discussed in Section II B, in the heavy quark mass limit it is possible to disregard internal motion of the quarks inside quarkonia, assuming that the momentum of the quarkonium is shared equally between the quarks, and disregard the difference of  $J/\psi$  and  $\eta_c$  masses, assuming  $M_{J/\psi} \approx M_\eta \approx 2m_Q$ . The evaluation of the partonic amplitudes requires computation of the Feynman diagrams shown in Figures 3, 4, and was done using FeynCalc package for *Mathematica* [91, 92]. This evaluation resembles similar studies of the single quarkonia photoproduction well-known from the literature [34–37]. Below we provide some technical details which might help to understand the main steps and assumptions needed for derivation of the final result.

Since GPDs are conventionally defined in the symmetric frame, we perform evaluation of the coefficient function in that frame, assuming that all momenta might be related using the transformations described in Section A. The momenta of partons (gluons) in this frame, before and after interaction, are given respectively by

$$k_{i,f} = \left( (x \pm \xi) \bar{P}^+, 0, \mathbf{k}_\perp \mp \frac{\Delta_\perp}{2} \right). \quad (\text{B1})$$

Furthermore, to simplify further notations, we will shift the rapidities of quarkonia and rewrite their momenta as

$$p_a = \left( e^{\tilde{y}_a} \bar{P}^+, \frac{(M_a^\perp)^2 e^{-\tilde{y}_a}}{2\bar{P}^+}, \mathbf{p}_a^\perp \right), \quad a = 1, 2, \quad (\text{B2})$$

$$\tilde{y}_a = -y_a + \ln(M_a^\perp/2\bar{P}^+). \quad (\text{B3})$$

This modification allows to suppress numerous factors  $\sim M_a^\perp/\bar{P}^+$ , so the coefficient functions will depend only on 2 dimensional variables,  $m_Q^2$  and  $Q^2$ . For example, the variable  $Z$  defined in (A7) will turn into a simple expression

$$Z = -2\xi + e^{\tilde{y}_1} + e^{\tilde{y}_2}. \quad (\text{B4})$$

Since we consider that formally both  $M_a$  and  $\bar{P}^+$  are large parameters of the same order, the variables  $y_a$  and  $\tilde{y}_a$  are also of the same order, and thus switching from  $y_a$  to  $\tilde{y}_a$  does not require modification of the underlying counting rules.

The chiral even gluon GPDs, which are expected to give the dominant contributions, are defined as [3, 34]

$$F^g(x, \xi, t) = \frac{1}{\bar{P}^+} \int \frac{dz}{2\pi} e^{ix\bar{P}^+} \left\langle P' \left| G^{+\mu a} \left( -\frac{z}{2} n \right) \mathcal{L} \left( -\frac{z}{2}, \frac{z}{2} \right) G_{\mu}^{+a} \left( \frac{z}{2} n \right) \right| P \right\rangle = \left( \bar{U}(P') \gamma_+ U(P) H^g(x, \xi, t) + \bar{U}(P') \frac{i\sigma^{+\alpha} \Delta_\alpha}{2m_N} U(P) E^g(x, \xi, t) \right), \quad (\text{B5})$$

$$\tilde{F}^g(x, \xi, t) = \frac{-i}{\bar{P}^+} \int \frac{dz}{2\pi} e^{ix\bar{P}^+} \left\langle P' \left| G^{+\mu a} \left( -\frac{z}{2} n \right) \mathcal{L} \left( -\frac{z}{2}, \frac{z}{2} \right) \tilde{G}_{\mu}^{+a} \left( \frac{z}{2} n \right) \right| P \right\rangle = \left( \bar{U}(P') \gamma_+ \gamma_5 U(P) \tilde{H}^g(x, \xi, t) + \bar{U}(P') \frac{\Delta^+ \gamma_5}{2m_N} U(P) \tilde{E}^g(x, \xi, t) \right). \quad (\text{B6})$$

$$\tilde{G}^{\mu\nu, a} \equiv \frac{1}{2} \varepsilon^{\mu\nu\alpha\beta} G_{\alpha\beta}^a, \quad \mathcal{L} \left( -\frac{z}{2}, \frac{z}{2} \right) \equiv \exp \left( i \int_{-z/2}^{z/2} d\zeta A^+(\zeta) \right). \quad (\text{B7})$$

where the skewedness variable  $\xi$  was defined in (30); for quarkonia pair production it might be expressed as a function of  $y_1, y_2, Q^2$ . In the light-cone gauge  $A^+ = 0$  we may rewrite the two-gluon operators in (B5, B6) as

$$G^{+\mu_\perp a}(z_1) G_{\mu_\perp}^{+a}(z_2) = g_{\mu\nu}^\perp (\partial^+ A^{\mu_\perp, a}(z_1)) (\partial^+ A^{\nu_\perp, a}(z_2)), \quad (\text{B8})$$

$$G^{+\mu_\perp a}(z_1) \tilde{G}_{\mu_\perp}^{+a}(z_2) = G^{+\mu_\perp a}(z_1) \tilde{G}_{-\mu_\perp}^a(z_2) = \frac{1}{2} \varepsilon_{-\mu_\perp \alpha \nu} G^{+\mu_\perp a}(z_1) G^{\alpha\nu, a}(z_2) = \varepsilon_{-\mu_\perp + \nu_\perp} G^{+\mu_\perp a}(z_1) G^{+\nu_\perp, a}(z_2) = \varepsilon_{\mu\nu}^\perp G^{+\mu, a}(z_1) G^{+\nu, a}(z_2). \quad (\text{B9})$$

After taking the integral over  $z$  in (B5, B6), we effectively switch to the momentum space, where the derivatives  $\partial_{z_1}^+$ ,  $\partial_{z_2}^+$  will turn into the factors  $k_{1,2}^+ \sim (x \pm \xi) \bar{P}^+$ , so we may rewrite (B5, B6) as [34]

$$\frac{1}{\bar{P}^+} \int \frac{dz}{2\pi} e^{ix\bar{P}^+} \left. - \langle P' \left| A_\mu^a \left( -\frac{z}{2}n \right) A_\nu^b \left( \frac{z}{2}n \right) \right| P \right\rangle \right|_{A^+=0 \text{ gauge}} = \frac{\delta^{ab}}{N_c^2 - 1} \left( \frac{-g_{\mu\nu}^\perp F^g(x, \xi, t) - \varepsilon_{\mu\nu}^\perp \tilde{F}^g(x, \xi, t)}{2(x - \xi + i0)(x + \xi - i0)} \right). \quad (\text{B10})$$

We may see that it is possible to extract the coefficient functions  $C_a$  and  $\tilde{C}_a$ , convoluting Lorentz indices of  $t$ -channel gluons in diagrams of Figures 3, 4 with  $g_{\mu\nu}^\perp$  and  $\varepsilon_{\mu\nu}^\perp$  respectively, and following [34] we assume that the variable  $\xi$  in denominator is always replaced as  $\xi \rightarrow \xi - i0$  in order to define proper contour deformation near the poles of the amplitude.

For evaluation of the coefficient functions, we also need to make proper projections of the  $\bar{Q}Q$  pairs onto the states with definite color and spins. According to potential models and NRQCD, the dominant Fock state in quarkonium is the color singlet  $\bar{Q}Q$  pair in  ${}^3S_1^{[1]}$  state for  $J/\psi$ , and  ${}^1S_0^{[1]}$  state for  $\eta_c$ . As discussed in [27, 28, 34], the projectors on color singlet and color octet states are given respectively by

$$\left( P^{[1]} \right)_{ij} = \frac{\delta_{ij}}{\sqrt{N_c}}, \quad \left( P_b^{[8]} \right)_{ij} = \sqrt{2} (t^b)_{ij}, \quad b = 1, \dots, 8. \quad (\text{B11})$$

The projections onto a state with definite total spin  $S$  and its projection  $S_z$  might be found using proper Clebsch-Gordan coefficients [27, 28, 34],

$$\begin{aligned} \hat{P}_{SS_z} &= \sum_{s_1, s_2} \left\langle \frac{1}{2} s_1 \frac{1}{2} s_2 \left| SS_z \right\rangle v \left( \frac{P}{2} - q, s_2 \right) \bar{u} \left( \frac{P}{2} + q, s_1 \right) = \\ &= \begin{cases} \frac{-1}{2\sqrt{2}} \left( \frac{\hat{P}}{2} - \hat{q} - m_Q \right) \gamma_5 \left( \frac{\hat{P}}{2} + \hat{q} + m_Q \right), & S = 0 \\ \frac{-1}{2\sqrt{2}} \left( \frac{\hat{P}}{2} - \hat{q} - m_Q \right) \hat{\varepsilon}_{J/\psi}(P) \left( \frac{\hat{P}}{2} + \hat{q} + m_Q \right), & S = 1 \end{cases} \end{aligned} \quad (\text{B12})$$

where  $P$  is the momentum of the produced quarkonium,  $q \approx 0$  is the momentum of relative motion of the quarks inside the quarkonium, and  $\varepsilon_{J/\psi}$  is the polarization vector of  $J/\psi$  mesons. Combining these projectors with proper color singlet LDMEs and disregarding momentum of the relative motion  $q$ , after some algebra we may obtain effective projectors of heavy quarks onto  $J/\psi$  and  $\eta_c$  states,

$$\left( \hat{V}_{\eta_c}^{[1]} \right)_{ij} = -\sqrt{\frac{\langle \mathcal{O}_{\eta_c}^{[1]} \rangle}{m_Q}} \frac{\delta_{ij}}{8N_c m_Q} \left( \frac{\hat{P}}{2} - \hat{q} - m_Q \right) \gamma_5 \left( \frac{\hat{P}}{2} + \hat{q} + m_Q \right) \approx -\sqrt{\frac{\langle \mathcal{O}_{\eta_c}^{[1]} \rangle}{m_Q}} \frac{\delta_{ij}}{4N_c} \left( \frac{\hat{P}}{2} - m_Q \right) \gamma_5 \quad (\text{B13})$$

$$\left( \hat{V}_{J/\psi}^{[1]} \right)_{ij} = -\sqrt{\frac{\langle \mathcal{O}_{J/\psi}^{[1]} \rangle}{m_Q}} \frac{\delta_{ij}}{8N_c m_Q} \left( \frac{\hat{P}}{2} - \hat{q} - m_Q \right) \hat{\varepsilon}_{J/\psi}(P) \left( \frac{\hat{P}}{2} + \hat{q} + m_Q \right) \approx \sqrt{\frac{\langle \mathcal{O}_{J/\psi}^{[1]} \rangle}{m_Q}} \frac{\delta_{ij}}{4N_c} \hat{\varepsilon}_{J/\psi}(P) \left( \frac{\hat{P}}{2} + m_Q \right) \quad (\text{B14})$$

where  $\langle \mathcal{O}_M^{[1]} \rangle$  are the corresponding color singlet long-distance matrix elements for  $J/\psi$  and  $\eta_c$  mesons. These objects can be related to the radial wave functions in potential model, and for the  $S$ -wave quarkonia [26, 34] this relation has a form

$$\langle \mathcal{O}_M^{[1]} \rangle = \frac{N_c}{2\pi} |R_S(0)|^2. \quad (\text{B15})$$

Phenomenological estimates, for example based on analysis of the partial decay width of  $J/\psi \rightarrow e^+e^-$ , suggest that  $\langle \mathcal{O}_{J/\psi}^{[1]} \left( {}^3S_1^{[1]} \right) \rangle \approx \langle \mathcal{O}_{\eta_c}^{[1]} \left( {}^1S_0^{[1]} \right) \rangle \approx 0.3 \text{ GeV}^3$  [84].

In evaluation of the diagrams from Figures 3, 4 we should take into account that each diagram should be accompanied with another diagram with permuted final state mesons  $1 \leftrightarrow 2$  (equivalently, diagram with inverted direction of quark lines), as well as a diagram with permutation of  $t$ -channel gluons, as shown in the Figure 12. The latter permutation gives contributions which differ only by change of the sign in front of the light-cone variable  $x$  and interchange of the Lorentz indices  $\mu \leftrightarrow \nu$ . According to (B10), we need to contract the free Lorentz indices  $\mu, \nu$  with symmetric  $g_{\mu\nu}^\perp$  or antisymmetric  $\varepsilon_{\mu\nu}^\perp$  in order to single out the contributions of  $F^g$  or  $\tilde{F}^g$ , for this reason eventually we conclude that the coefficient functions  $C_a$ ,  $\tilde{C}_a$  will be even or odd functions of the variable  $x$  respectively. Since we disregard internal motion of quarks inside quarkonia, the momenta of all partons are fixed by energy-momentum conservation and could be expressed as linear combinations of the momenta of the quarkonia and  $t$ -channel gluons. Taking into account (B10, B13, B14), we may obtain for the coefficient functions



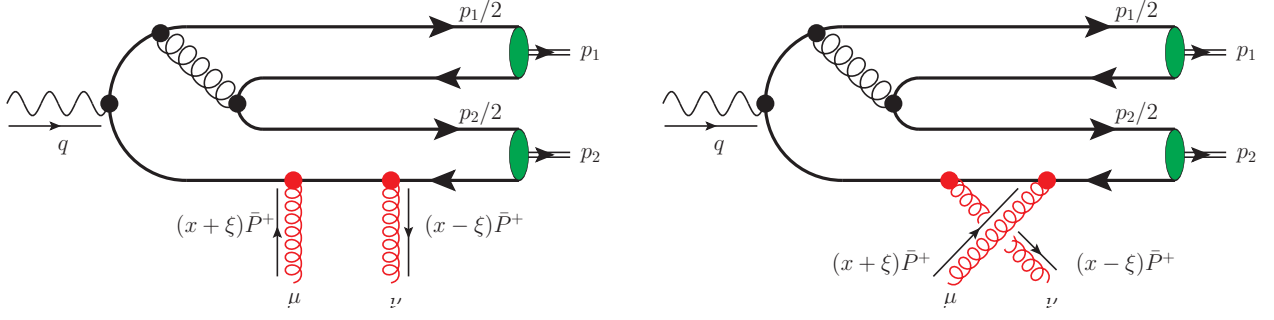


Figure 12. Schematic illustration of the diagrams with direct and permuted  $t$ -channel gluons, which are related to each other by inversion of sign in front of light-cone fraction  $x \leftrightarrow -x$ , and permutation of the Lorentz indices  $\mu \leftrightarrow \nu$ .

$$C_a(x, \tilde{y}_1, \tilde{y}_2) = \kappa \frac{\mathcal{C}_a(x, \tilde{y}_1, \tilde{y}_2) + \mathcal{C}_a(-x, \tilde{y}_1, \tilde{y}_2)}{(x - \xi + i0)(x + \xi - i0)} \quad (\text{B16})$$

$$\tilde{\mathcal{C}}_a(x, \tilde{y}_1, \tilde{y}_2) = \kappa \frac{\tilde{\mathcal{C}}_a(x, \tilde{y}_1, \tilde{y}_2) - \tilde{\mathcal{C}}_a(-x, \tilde{y}_1, \tilde{y}_2)}{(x - \xi + i0)(x + \xi - i0)} \quad (\text{B17})$$

where the constant  $\kappa$  is defined as

$$\kappa = (4\pi\alpha_s)^2 e_Q \frac{\sqrt{\langle \mathcal{O}_{J/\psi}^{[1]}(3S_1^{[1]}) \rangle \langle \mathcal{O}_{\eta_c}^{[1]}(1S_0^{[1]}) \rangle}}{4N_c^2 m_Q} \left( \varepsilon_{J/\psi}^* \cdot \varepsilon_T^{(\gamma)} \right), \quad (\text{B18})$$

and the factors  $x \pm \xi \mp i0$  in denominators of (B16, B17) stem from (B10). The contribution of each diagram from the Figures 3, 4 to functions  $\mathcal{C}_a$  and  $\tilde{\mathcal{C}}_a$  might be obtained taking Dirac and color traces over the heavy quark loop, and contracting free Lorentz indices  $\mu, \nu$  with  $g_{\mu\nu}^\perp$  or  $\varepsilon_{\mu\nu}^\perp$  respectively; this operation was done using FeynCalc package for *Mathematica* [91, 92]. We need to mention that gluon GPDs  $H^g, E^g$  are even functions of variable  $x$ , whereas  $\tilde{H}^g, \tilde{E}^g$  are odd functions [3], for this reason in convolution over  $x$  both terms in numerators of (B16, B17) give equal nonzero contributions. Numerically the dominant contribution comes from GPD  $H^g$ , whereas contribution of  $\tilde{H}^g$  is negligibly small. As we will see below, the functions  $\mathcal{C}_a, \tilde{\mathcal{C}}_a$  might have other poles as a function of  $x$ , so the structure of the functions  $\mathcal{C}_a, \tilde{\mathcal{C}}_a$  might be represented schematically as a sum (37).

The explicit expressions for the functions  $\mathcal{C}_a, \tilde{\mathcal{C}}_a$  depend on polarizations of the photon and are given by

$$\mathcal{C}_L = \mathcal{O}(p_{a\perp}/Q, p_{a\perp}/m_Q) \approx 0 \quad (\text{B19})$$

$$\mathcal{C}_T = \frac{N_c^2 - 1}{4N_c} \sum_{k=1}^7 a_k - \frac{1}{4N_c} \sum_{k=1}^3 b_k + \frac{N_c}{4} \sum_{k=1}^5 c_k + \frac{1}{4} \sum_{k=1}^2 d_k \quad (\text{B20})$$

$$\tilde{\mathcal{C}}_T = \frac{N_c^2 - 1}{4N_c} \sum_{k=1}^7 \tilde{a}_k - \frac{1}{4N_c} \sum_{k=1}^3 \tilde{b}_k + \frac{N_c}{4} \sum_{k=1}^5 \tilde{c}_k + \frac{1}{4} \sum_{k=1}^2 \tilde{d}_k \quad (\text{B21})$$

where the contributions  $a_i, b_i, \tilde{a}_i, \tilde{b}_i$  stem from the diagrams without 3-gluon vertices in the Figure 3, the terms  $c_i, \tilde{c}_i$  come from the diagrams which include at least one three-gluon vertex, and the terms  $d_i, \tilde{d}_i$  stem from the diagrams in the Figure 4. Explicitly, these contributions are given by

$$\begin{aligned} a_1 &= 4e^{\tilde{y}_1 + \tilde{y}_2} Z (e^{\tilde{y}_1 + \tilde{y}_2} Q^2 + 4(e^{\tilde{y}_1} + e^{\tilde{y}_2}) m_Q^2 Z) (x + \xi) \times \\ &\times \left[ m_Q (4e^{\tilde{y}_1} m_Q^2 (e^{\tilde{y}_1} - Z) Z + (e^{2\tilde{y}_2} + 2e^{\tilde{y}_2} (e^{\tilde{y}_1} - Z)) (e^{\tilde{y}_1} Q^2 + 4m_Q^2 Z)) \times \right. \\ &((e^{\tilde{y}_1} Q^2 + 4m_Q^2 Z) (e^{2\tilde{y}_2} + 2e^{\tilde{y}_2} (e^{\tilde{y}_1} - x - Z - \xi)) + 4e^{\tilde{y}_1} m_Q^2 Z (e^{\tilde{y}_1} - x - Z - \xi)) \\ &\left. \times (1 + \cosh(\tilde{y}_1 - \tilde{y}_2)) \right]^{-1}, \end{aligned} \quad (\text{B22})$$

$$a_2 = \frac{2e^{2\tilde{y}_2} (e^{\tilde{y}_1} + e^{\tilde{y}_2}) Z (e^{\tilde{y}_1 + \tilde{y}_2} Q^2 + 4m_Q^2 Z^2)}{m_Q (e^{\tilde{y}_1} + e^{\tilde{y}_2} - 2Z) \left( e^{\tilde{y}_1 + \tilde{y}_2} Q^2 + 2(e^{\tilde{y}_1} + e^{\tilde{y}_2}) m_Q^2 Z \right) \left( -e^{2\tilde{y}_2} Q^2 + e^{\tilde{y}_2} Q^2 Z + 4m_Q^2 Z^2 \right) \xi}, \quad (\text{B23})$$

$$a_3 = 8e^{\tilde{y}_1 + \tilde{y}_2} Z (e^{\tilde{y}_1 + 2\tilde{y}_2} Q^2 - 8e^{\tilde{y}_1} m_Q^2 Z^2 - 2e^{\tilde{y}_2} Z (e^{\tilde{y}_1} Q^2 + 2m_Q^2 Z)) \times \\ \times \left[ (e^{\tilde{y}_1} + e^{\tilde{y}_2}) m_Q (e^{2\tilde{y}_2} Q^2 - e^{\tilde{y}_2} Q^2 Z - 4m_Q^2 Z^2) \right. \\ \left. \times \left( (2e^{\tilde{y}_2} + e^{\tilde{y}_1} - 2Z) e^{\tilde{y}_1 + \tilde{y}_2} Q^2 + 4m_Q^2 Z (e^{\tilde{y}_1} (e^{\tilde{y}_1} - 2Z) + e^{2\tilde{y}_2} - e^{\tilde{y}_2} (Z - 2e^{\tilde{y}_1})) \right) \right]^{-1}, \quad (\text{B24})$$

$$a_4 = -8e^{\tilde{y}_1 + 2\tilde{y}_2} Z (e^{\tilde{y}_1 + \tilde{y}_2} Q^2 + 4m_Q^2 Z^2) \times \\ \times \left[ m_Q (e^{\tilde{y}_1} + e^{\tilde{y}_2} - 2Z) (e^{2\tilde{y}_2} Q^2 - 2e^{\tilde{y}_2} Q^2 Z - 4m_Q^2 Z^2) \right. \\ \left. \times \left( (2e^{\tilde{y}_2} + e^{\tilde{y}_1} - 2Z) e^{\tilde{y}_1 + \tilde{y}_2} Q^2 + 4m_Q^2 Z (e^{\tilde{y}_1} (e^{\tilde{y}_1} - 2Z) + e^{2\tilde{y}_2} - e^{\tilde{y}_2} (Z - 2e^{\tilde{y}_1})) \right) \right]^{-1}, \quad (\text{B25})$$

$$a_5 = 8e^{2(\tilde{y}_1 + \tilde{y}_2)} Q^2 Z (e^{\tilde{y}_1 + \tilde{y}_2} Q^2 + 4m_Q^2 Z(-x + Z + \xi)) \times \\ \times \left[ m_Q (e^{\tilde{y}_1 + \tilde{y}_2} Q^2 + 2(e^{\tilde{y}_1} + e^{\tilde{y}_2}) m_Q^2 Z) (-e^{2\tilde{y}_2} Q^2 + 2e^{\tilde{y}_2} Q^2 Z + 4m_Q^2 Z^2) \times \right. \\ \left. \times (e^{\tilde{y}_1} + e^{\tilde{y}_2} + 2x - 2Z - 2\xi) (-e^{2\tilde{y}_1} Q^2 - 2e^{\tilde{y}_1} Q^2(x - Z - \xi) + 4m_Q^2 Z(-x + Z + \xi)) \right]^{-1}, \quad (\text{B26})$$

$$a_6 = 16e^{\tilde{y}_1 + 2\tilde{y}_2} m_Q Z^2 (Q^2 e^{\tilde{y}_2} (e^{2\tilde{y}_2} - 2e^{\tilde{y}_1} Z + e^{\tilde{y}_2} (e^{\tilde{y}_1} - 2(x + Z + \xi))) - 4m_Q^2 Z^2 (e^{\tilde{y}_1} + e^{\tilde{y}_2})) \times \\ \times \left[ (e^{\tilde{y}_1 + \tilde{y}_2} Q^2 + 2(e^{\tilde{y}_1} + e^{\tilde{y}_2}) m_Q^2 Z) (e^{2\tilde{y}_2} Q^2 - 2e^{\tilde{y}_2} Q^2 Z - 4m_Q^2 Z^2) (e^{\tilde{y}_1} + e^{\tilde{y}_2} - 2(x + Z + \xi)) \times \right. \\ \left. \times (e^{2\tilde{y}_2} (e^{\tilde{y}_1} Q^2 + 4m_Q^2 Z) + 4e^{\tilde{y}_1} m_Q^2 Z (e^{\tilde{y}_1} - x - Z - \xi) + 2e^{\tilde{y}_2} (e^{\tilde{y}_1} Q^2 + 4m_Q^2 Z) (e^{\tilde{y}_1} - x - Z - \xi)) \right]^{-1}, \quad (\text{B27})$$

$$a_7 = \frac{4e^{2\tilde{y}_2} Q^2 Z(x + \xi)}{m_Q \left( 2e^{\tilde{y}_2} Q^2 Z - e^{2\tilde{y}_2} Q^2 + 4m_Q^2 Z^2 \right) \left( 2e^{\tilde{y}_2} Q^2 (x + Z + \xi) - e^{2\tilde{y}_2} Q^2 + 4m_Q^2 Z(x + Z + \xi) \right) (1 + \cosh(\tilde{y}_1 - \tilde{y}_2))}, \quad (\text{B28})$$

$$b_1 = \frac{-8e^{3\tilde{y}_1 + \tilde{y}_2} Q^2 Z}{m_Q \left( e^{\tilde{y}_1 + \tilde{y}_2} Q^2 + 2(e^{\tilde{y}_1} + e^{\tilde{y}_2}) m_Q^2 Z \right) \left( e^{2\tilde{y}_1} Q^2 - 2e^{\tilde{y}_1} Q^2 Z - 4m_Q^2 Z^2 \right) (e^{\tilde{y}_1} + e^{\tilde{y}_2} + 2x - 2Z - 2\xi)}, \quad (\text{B29})$$

$$b_2 = -\frac{4e^{\tilde{y}_1 + \tilde{y}_2} (e^{\tilde{y}_1} Q^2 + 2m_Q^2 Z)}{(e^{\tilde{y}_1} + e^{\tilde{y}_2}) m_Q^3 \left( e^{2\tilde{y}_1} Q^2 - 2e^{\tilde{y}_1} Q^2 (x + Z + \xi) - 4m_Q^2 Z(x + Z + \xi) \right)}, \quad (\text{B30})$$

$$b_3 = \frac{1}{(e^{\tilde{y}_1} + e^{\tilde{y}_2}) m_Q} \times \\ \times \frac{8e^{\tilde{y}_1 + \tilde{y}_2} Z (-e^{3\tilde{y}_1} Q^2 - e^{2\tilde{y}_1 + \tilde{y}_2} Q^2 + 2e^{\tilde{y}_1 + \tilde{y}_2} Q^2 Z + 2e^{2\tilde{y}_1} Q^2 (x + Z + \xi) + 4m_Q^2 Z^2 (e^{\tilde{y}_1} + e^{\tilde{y}_2}))}{\left( Q^2 (e^{2\tilde{y}_1} - 2e^{\tilde{y}_1} Z) - 4m_Q^2 Z^2 \right) (e^{\tilde{y}_1} + e^{\tilde{y}_2} + 2x - 2\xi) \left( Q^2 (e^{2\tilde{y}_1} - 2e^{\tilde{y}_1} (x + Z + \xi)) - 4m_Q^2 Z(x + Z + \xi) \right)}, \quad (\text{B31})$$

$$\begin{aligned}
c_1 = & 2e^{2\tilde{y}_1+\tilde{y}_2} \left[ e^{4\tilde{y}_2}(-3x+\xi) - 2e^{3\tilde{y}_2} (e^{\tilde{y}_1}(6x-2\xi) + \xi(-5x+\xi)) \right. \\
& + e^{2\tilde{y}_1} (e^{\tilde{y}_1}-4\xi) (2(x-\xi)\xi + e^{\tilde{y}_1}(-3x+\xi)) \\
& - 2e^{\tilde{y}_1+\tilde{y}_2} (e^{2\tilde{y}_1}(6x-2\xi) + e^{\tilde{y}_1}\xi(-19x+7\xi) + 2\xi(-2x^2+5x\xi+\xi^2)) \\
& \left. - 2e^{2\tilde{y}_2} (e^{2\tilde{y}_1}(9x-3\xi) + e^{\tilde{y}_1}\xi(-17x+5\xi) + 4\xi(x^2+x\xi-\xi^2)) \right] \times \\
& \times \left[ (e^{\tilde{y}_1}+e^{\tilde{y}_2})^2 m_Q^3 (e^{2\tilde{y}_2}+e^{\tilde{y}_1}(e^{\tilde{y}_1}-2\xi) + 2e^{\tilde{y}_2}(e^{\tilde{y}_1}-2\xi)) \times \right. \\
& \left. \times (e^{2\tilde{y}_2}+e^{\tilde{y}_1}(e^{\tilde{y}_1}-4\xi) + 2e^{\tilde{y}_2}(e^{\tilde{y}_1}-\xi)) (x-\xi) (e^{\tilde{y}_1}+e^{\tilde{y}_2}-2(x+\xi)) \right]^{-1},
\end{aligned} \tag{B32}$$

$$\begin{aligned}
c_2 = & -2e^{\tilde{y}_1+\tilde{y}_2} \left[ e^{5\tilde{y}_1}(x-3\xi) + e^{3\tilde{y}_2}(e^{\tilde{y}_2}-4\xi)(e^{\tilde{y}_2}-2\xi)(-x+\xi) \right. \\
& + 2e^{3\tilde{y}_1}(e^{2\tilde{y}_2}(x-7\xi) - 2e^{\tilde{y}_2}(5x-11\xi)\xi + 12(x-\xi)\xi^2) + e^{4\tilde{y}_1}(e^{\tilde{y}_2}(3x-11\xi) + 2\xi(-5x+9\xi)) \\
& + e^{\tilde{y}_1+2\tilde{y}_2}(4e^{\tilde{y}_2}(3x-\xi)\xi + e^{2\tilde{y}_2}(-3x+\xi) - 4\xi(-2x^2+3x\xi+\xi^2)) \\
& \left. - 2e^{2\tilde{y}_1+\tilde{y}_2}(2e^{\tilde{y}_2}(x-7\xi)\xi + e^{2\tilde{y}_2}(x+3\xi) + 2\xi(2x^2-5x\xi+7\xi^2)) \right] \times \\
& \times \left[ (e^{\tilde{y}_1}+e^{\tilde{y}_2}) m_Q^3 (e^{2\tilde{y}_2}+e^{\tilde{y}_1}(e^{\tilde{y}_1}-2\xi) + 2e^{\tilde{y}_2}(e^{\tilde{y}_1}-2\xi)) (e^{\tilde{y}_1}+e^{\tilde{y}_2}-4\xi) \times \right. \\
& \left. \times (e^{2\tilde{y}_2}+e^{\tilde{y}_1}(e^{\tilde{y}_1}-4\xi) + 2e^{\tilde{y}_2}(e^{\tilde{y}_1}-\xi)) (e^{\tilde{y}_1}+e^{\tilde{y}_2}+2x-2\xi)(x-\xi) \right]^{-1},
\end{aligned} \tag{B33}$$

$$c_3 = \frac{2e^{2\tilde{y}_1+\tilde{y}_2} (2e^{2\tilde{y}_1} + 2e^{2\tilde{y}_2} + 4e^{\tilde{y}_1+\tilde{y}_2} - 2e^{\tilde{y}_1}(x+\xi) - e^{\tilde{y}_2}(x+\xi))}{(e^{\tilde{y}_1}+e^{\tilde{y}_2})^2 m_Q^3 (e^{\tilde{y}_1}+e^{\tilde{y}_2}-2(x+\xi)) (e^{2\tilde{y}_1}+e^{2\tilde{y}_2}+2e^{\tilde{y}_1+\tilde{y}_2}-2e^{\tilde{y}_1}(x+\xi)-e^{\tilde{y}_2}(x+\xi))}, \tag{B34}$$

$$\begin{aligned}
c_4 = & -\frac{2e^{2(\tilde{y}_1+\tilde{y}_2)}}{(e^{\tilde{y}_1}+e^{\tilde{y}_2})^2 m_Q^3 (e^{\tilde{y}_1}+e^{\tilde{y}_2}-2(x+\xi))} \times \\
& \times \left[ \frac{4e^{2\tilde{y}_1}\xi + 4e^{2\tilde{y}_2}\xi + 8e^{\tilde{y}_1+\tilde{y}_2}\xi - 4e^{\tilde{y}_1}\xi(x+\xi) - 2e^{\tilde{y}_2}(x+\xi)(x+3\xi)}{(e^{2\tilde{y}_2}+e^{\tilde{y}_1}(e^{\tilde{y}_1}-2\xi) + 2e^{\tilde{y}_2}(e^{\tilde{y}_1}-2\xi)) (e^{2\tilde{y}_1}+e^{2\tilde{y}_2}+2e^{\tilde{y}_1+\tilde{y}_2}-e^{\tilde{y}_1}(x+\xi)-2e^{\tilde{y}_2}(x+\xi))} \right. \\
& \left. - \frac{(x+\xi)(e^{2\tilde{y}_2}+2e^{\tilde{y}_2}(e^{\tilde{y}_1}-\xi) + e^{\tilde{y}_1}(e^{\tilde{y}_1}-2(x+\xi)))}{(e^{2\tilde{y}_2}+e^{\tilde{y}_1}(e^{\tilde{y}_1}-4\xi) + 2e^{\tilde{y}_2}(e^{\tilde{y}_1}-\xi)) (e^{2\tilde{y}_1}+e^{2\tilde{y}_2}+2e^{\tilde{y}_1+\tilde{y}_2}-2e^{\tilde{y}_1}(x+\xi)-e^{\tilde{y}_2}(x+\xi))} \right],
\end{aligned} \tag{B35}$$

$$c_5 = \frac{2e^{\tilde{y}_1+2\tilde{y}_2} (5(e^{\tilde{y}_1}+e^{\tilde{y}_2}) + 4(x+4\xi))}{(e^{\tilde{y}_1}+e^{\tilde{y}_2})^2 m_Q^3 (e^{\tilde{y}_1}+e^{\tilde{y}_2}+4\xi) (e^{\tilde{y}_1}+e^{\tilde{y}_2}+2x+6\xi)}, \tag{B36}$$

$$\begin{aligned}
d_1 = & -4e^{\tilde{y}_1+\tilde{y}_2} Z (e^{\tilde{y}_1+2\tilde{y}_2} Q^2 - 4e^{\tilde{y}_1} m_Q^2 Z^2 + e^{\tilde{y}_2} (-e^{2\tilde{y}_1} Q^2 + 4m_Q^2 Z^2 + e^{\tilde{y}_1} Q^2(x-2Z+\xi))) \times \\
& \times \left[ m_Q (2e^{\tilde{y}_2} Q^2 Z - e^{2\tilde{y}_2} Q^2 + 4m_Q^2 Z^2) (e^{\tilde{y}_1} - x - \xi) \times \right. \\
& \left. \times (e^{2\tilde{y}_2} (e^{\tilde{y}_1} Q^2 - 4m_Q^2 Z) - 4e^{\tilde{y}_1} m_Q^2 Z (e^{\tilde{y}_1} - x + Z - \xi) - 2e^{\tilde{y}_2} (e^{\tilde{y}_1} Q^2 - 4m_Q^2 Z) (e^{\tilde{y}_1} - x + Z - \xi)) \right]^{-1},
\end{aligned} \tag{B37}$$

$$d_2 = -\frac{8e^{\tilde{y}_1+\tilde{y}_2} Z (e^{2\tilde{y}_2} Q^2 - 4m_Q^2 Z^2 - e^{\tilde{y}_2} Q^2(x+2Z+\xi))}{m_Q (2e^{\tilde{y}_2} Q^2 Z - e^{2\tilde{y}_2} Q^2 + 4m_Q^2 Z^2) (e^{\tilde{y}_1} - x - \xi) (2e^{\tilde{y}_2} Q^2(x+Z+\xi) - e^{2\tilde{y}_2} Q^2 + 4m_Q^2 Z(x+Z+\xi))}, \tag{B38}$$

$$\begin{aligned}
\tilde{a}_1 = & 8e^{2(\tilde{y}_1+\tilde{y}_2)} Z (e^{\tilde{y}_1+\tilde{y}_2} Q^2 + 4e^{\tilde{y}_1} m_Q^2 Z + 4e^{\tilde{y}_2} m_Q^2 Z) (x+\xi) \times \\
& \times \left[ (e^{\tilde{y}_1}+e^{\tilde{y}_2})^2 m_Q \times \right. \\
& \times (e^{2\tilde{y}_2} (e^{\tilde{y}_1} Q^2 + 4m_Q^2 Z) + 4e^{\tilde{y}_1} m_Q^2 Z (e^{\tilde{y}_1} - x - Z - \xi) + 2e^{\tilde{y}_2} (e^{\tilde{y}_1} Q^2 + 4m_Q^2 Z) (e^{\tilde{y}_1} - x - Z - \xi)) \\
& \left. \times (e^{2\tilde{y}_2} (e^{\tilde{y}_1} Q^2 + 4m_Q^2 Z) + 2e^{\tilde{y}_2} (e^{\tilde{y}_1} - Z) (e^{\tilde{y}_1} Q^2 + 4m_Q^2 Z) + 4e^{\tilde{y}_1} m_Q^2 (e^{\tilde{y}_1} - Z) Z) \right]^{-1},
\end{aligned} \tag{B39}$$

$$\tilde{a}_2 = \frac{2e^{2\tilde{y}_2} (e^{\tilde{y}_1} + e^{\tilde{y}_2}) Z (e^{\tilde{y}_1+\tilde{y}_2} Q^2 + 4m_Q^2 Z^2)}{m_Q (e^{\tilde{y}_1} + e^{\tilde{y}_2} - 2Z) (e^{\tilde{y}_1+\tilde{y}_2} Q^2 + 2m_Q^2 Z (e^{\tilde{y}_1} + e^{\tilde{y}_2})) (e^{2\tilde{y}_2} Q^2 - 2e^{\tilde{y}_2} Q^2 Z - 4m_Q^2 Z^2)} \xi, \quad (\text{B40})$$

$$\begin{aligned} \tilde{a}_3 &= 8e^{\tilde{y}_1+\tilde{y}_2} Z (e^{\tilde{y}_1+2\tilde{y}_2} Q^2 - 8e^{\tilde{y}_1} m_Q^2 Z^2 - 2e^{\tilde{y}_2} Z (e^{\tilde{y}_1} Q^2 + 2m_Q^2 Z)) \times \\ &\times \left[ (e^{\tilde{y}_1} + e^{\tilde{y}_2}) m_Q (e^{2\tilde{y}_2} Q^2 - 2e^{\tilde{y}_2} Q^2 Z - 4m_Q^2 Z^2) \times \right. \\ &\times \left. (4e^{\tilde{y}_1} m_Q^2 (e^{\tilde{y}_1} - 2Z) Z + 2e^{2\tilde{y}_2} (e^{\tilde{y}_1} Q^2 + 2m_Q^2 Z) + e^{\tilde{y}_2} (e^{2\tilde{y}_1} Q^2 - 2e^{\tilde{y}_1} (-4m_Q^2 + Q^2) Z - 4m_Q^2 Z^2)) \right]^{-1}, \end{aligned} \quad (\text{B41})$$

$$\begin{aligned} \tilde{a}_4 &= 8e^{\tilde{y}_1+2\tilde{y}_2} Z (e^{\tilde{y}_1+\tilde{y}_2} Q^2 + 4m_Q^2 Z^2) \times \\ &\times \left[ m_Q (e^{\tilde{y}_1} + e^{\tilde{y}_2} - 2Z) (e^{2\tilde{y}_2} Q^2 - 2e^{\tilde{y}_2} Q^2 Z - 4m_Q^2 Z^2) \times \right. \\ &\times \left. (4e^{\tilde{y}_1} m_Q^2 (e^{\tilde{y}_1} - 2Z) Z + 2e^{2\tilde{y}_2} (e^{\tilde{y}_1} Q^2 + 2m_Q^2 Z) + e^{\tilde{y}_2} (e^{2\tilde{y}_1} Q^2 - 2e^{\tilde{y}_1} (-4m_Q^2 + Q^2) Z - 4m_Q^2 Z^2)) \right]^{-1}, \end{aligned} \quad (\text{B42})$$

$$\begin{aligned} \tilde{a}_5 &= 8e^{2(\tilde{y}_1+\tilde{y}_2)} Q^2 Z (e^{\tilde{y}_1+\tilde{y}_2} Q^2 + 4m_Q^2 Z(-x + Z + \xi)) \times \\ &\times \left[ m_Q (e^{\tilde{y}_1+\tilde{y}_2} Q^2 + 2m_Q^2 Z (e^{\tilde{y}_1} + e^{\tilde{y}_2})) (-e^{2\tilde{y}_2} Q^2 + 2e^{\tilde{y}_2} Q^2 Z + 4m_Q^2 Z^2) \times \right. \\ &\times \left. (e^{\tilde{y}_1} + e^{\tilde{y}_2} + 2x - 2Z - 2\xi) (-e^{2\tilde{y}_1} Q^2 - 2e^{\tilde{y}_1} Q^2(x - Z - \xi) + 4m_Q^2 Z(-x + Z + \xi)) \right]^{-1}, \end{aligned} \quad (\text{B43})$$

$$\begin{aligned} \tilde{a}_6 &= -16e^{\tilde{y}_1+2\tilde{y}_2} m_Q Z^2 (e^{3\tilde{y}_2} Q^2 - 4e^{\tilde{y}_1} m_Q^2 Z^2 - 2e^{\tilde{y}_2} Z (e^{\tilde{y}_1} Q^2 + 2m_Q^2 Z) + e^{2\tilde{y}_2} Q^2 (e^{\tilde{y}_1} - 2(x + Z + \xi))) \times \\ &\times \left[ (e^{\tilde{y}_1+\tilde{y}_2} Q^2 + 2m_Q^2 Z (e^{\tilde{y}_1} + e^{\tilde{y}_2})) (e^{2\tilde{y}_2} Q^2 - 2e^{\tilde{y}_2} Q^2 Z - 4m_Q^2 Z^2) \times \right. \\ &\times (e^{2\tilde{y}_2} (e^{\tilde{y}_1} Q^2 + 4m_Q^2 Z) + 4e^{\tilde{y}_1} m_Q^2 Z (e^{\tilde{y}_1} - x - Z - \xi) + 2e^{\tilde{y}_2} (e^{\tilde{y}_1} Q^2 + 4m_Q^2 Z) (e^{\tilde{y}_1} - x - Z - \xi)) \\ &\times \left. (e^{\tilde{y}_1} + e^{\tilde{y}_2} - 2(x + Z + \xi)) \right]^{-1}, \end{aligned} \quad (\text{B44})$$

$$\tilde{a}_7 = -\frac{8e^{\tilde{y}_1+3\tilde{y}_2} Q^2 Z(x + \xi)}{(e^{\tilde{y}_1} + e^{\tilde{y}_2})^2 m_Q (e^{2\tilde{y}_2} Q^2 - 2e^{\tilde{y}_2} Q^2 Z - 4m_Q^2 Z^2) (e^{2\tilde{y}_2} Q^2 - 2e^{\tilde{y}_2} Q^2(x + Z + \xi) - 4m_Q^2 Z(x + Z + \xi))}, \quad (\text{B45})$$

$$\tilde{b}_1 = \frac{8e^{3\tilde{y}_1+\tilde{y}_2} Q^2 Z}{m_Q (e^{\tilde{y}_1+\tilde{y}_2} Q^2 + 2m_Q^2 Z (e^{\tilde{y}_1} + e^{\tilde{y}_2})) (e^{2\tilde{y}_1} Q^2 - 2e^{\tilde{y}_1} Q^2 Z - 4m_Q^2 Z^2) (e^{\tilde{y}_1} + e^{\tilde{y}_2} + 2x - 2Z - 2\xi)}, \quad (\text{B46})$$

$$\tilde{b}_2 = \frac{4e^{\tilde{y}_1+\tilde{y}_2} (e^{\tilde{y}_1} Q^2 + 2m_Q^2 Z)}{(e^{\tilde{y}_1} + e^{\tilde{y}_2}) m_Q^3 (e^{2\tilde{y}_1} Q^2 - 2e^{\tilde{y}_1} Q^2(x + Z + \xi) - 4m_Q^2 Z(x + Z + \xi))}, \quad (\text{B47})$$

$$\tilde{b}_3 = \frac{8e^{\tilde{y}_1+\tilde{y}_2} Z (e^{3\tilde{y}_1} Q^2 + e^{2\tilde{y}_1+\tilde{y}_2} Q^2 - 2e^{\tilde{y}_1+\tilde{y}_2} Q^2 Z - 4(e^{\tilde{y}_1} + e^{\tilde{y}_2}) m_Q^2 Z^2 - 2e^{2\tilde{y}_1} Q^2(x + Z + \xi)) (e^{\tilde{y}_1} + e^{\tilde{y}_2})^{-1}}{m_Q (e^{2\tilde{y}_1} Q^2 - 2e^{\tilde{y}_1} Q^2 Z - 4m_Q^2 Z^2) (e^{\tilde{y}_1} + e^{\tilde{y}_2} + 2x - 2\xi) (Q^2 (e^{2\tilde{y}_1} - 2e^{\tilde{y}_1}(x + Z + \xi)) - 4m_Q^2 Z(x + Z + \xi))}, \quad (\text{B48})$$

$$\begin{aligned} \tilde{c}_1 &= -2e^{2\tilde{y}_1+\tilde{y}_2} \left[ e^{4\tilde{y}_2} + e^{2\tilde{y}_1} (e^{\tilde{y}_1} - 4\xi) (e^{\tilde{y}_1} - 2\xi) + 4e^{3\tilde{y}_2} (e^{\tilde{y}_1} - \xi) + \right. \\ &\quad \left. + 2e^{2\tilde{y}_2} (3e^{2\tilde{y}_1} - 7e^{\tilde{y}_1} \xi - 2\xi(2x + \xi)) + 4e^{\tilde{y}_1+\tilde{y}_2} (e^{2\tilde{y}_1} - 4e^{\tilde{y}_1} \xi + \xi(2x + 5\xi)) \right] \times \\ &\times \left[ (e^{\tilde{y}_1} + e^{\tilde{y}_2})^2 m_Q^3 (e^{2\tilde{y}_2} + e^{\tilde{y}_1} (e^{\tilde{y}_1} - 2\xi) + 2e^{\tilde{y}_2} (e^{\tilde{y}_1} - 2\xi)) \times \right. \\ &\times \left. (e^{2\tilde{y}_2} + e^{\tilde{y}_1} (e^{\tilde{y}_1} - 4\xi) + 2e^{\tilde{y}_2} (e^{\tilde{y}_1} - \xi)) (e^{\tilde{y}_1} + e^{\tilde{y}_2} - 2(x + \xi)) \right]^{-1}, \end{aligned}$$

$$\begin{aligned}
\tilde{c}_2 = & -2e^{\tilde{y}_1+\tilde{y}_2} \left[ e^{5\tilde{y}_1} + e^{4\tilde{y}_1} (5e^{\tilde{y}_2} - 6\xi) + e^{3\tilde{y}_2} (e^{\tilde{y}_2} - 4\xi) (e^{\tilde{y}_2} - 2\xi) \right. \\
& + 2e^{3\tilde{y}_1} (5e^{2\tilde{y}_2} + e^{\tilde{y}_2}(4x - 9\xi) + 4\xi^2) \\
& + e^{\tilde{y}_1+2\tilde{y}_2} (5e^{2\tilde{y}_2} + 2e^{\tilde{y}_2}(4x - 9\xi) + 8\xi(-3x + \xi)) \\
& \left. + 2e^{2\tilde{y}_1+\tilde{y}_2} (5e^{2\tilde{y}_2} + 4e^{\tilde{y}_2}(2x - 3\xi) + 6\xi(-2x + \xi)) \right] \times \\
& \times \left[ (e^{\tilde{y}_1} + e^{\tilde{y}_2}) m_Q^3 (e^{2\tilde{y}_2} + e^{\tilde{y}_1} (e^{\tilde{y}_1} - 2\xi) + 2e^{\tilde{y}_2} (e^{\tilde{y}_1} - 2\xi)) \times \right. \\
& \left. \times (e^{2\tilde{y}_2} + e^{\tilde{y}_1} (e^{\tilde{y}_1} - 4\xi) + 2e^{\tilde{y}_2} (e^{\tilde{y}_1} - \xi)) (e^{\tilde{y}_1} + e^{\tilde{y}_2} - 4\xi) (e^{\tilde{y}_1} + e^{\tilde{y}_2} + 2x - 2\xi) \right]^{-1}, \tag{B49}
\end{aligned}$$

$$\begin{aligned}
\tilde{c}_3 = & 4e^{\tilde{y}_1+\tilde{y}_2} \left[ e^{5\tilde{y}_1} + e^{4\tilde{y}_1} (5e^{\tilde{y}_2} + x - 5\xi) + e^{\tilde{y}_1+2\tilde{y}_2} (5e^{\tilde{y}_2} + 2(x - 7\xi)) (e^{\tilde{y}_2} - 2\xi) \right. \\
& + e^{3\tilde{y}_2} (e^{\tilde{y}_2} + x - 3\xi) (e^{\tilde{y}_2} - 2\xi) + 2e^{2\tilde{y}_1+\tilde{y}_2} (5e^{2\tilde{y}_2} + e^{\tilde{y}_2}(x - 19\xi) - 2(x - 8\xi)\xi) \\
& \left. + 2e^{3\tilde{y}_1} (5e^{2\tilde{y}_2} + e^{\tilde{y}_2}(x - 12\xi) + \xi(-x + 3\xi)) \right] \times \\
& \times \left[ (e^{\tilde{y}_1} + e^{\tilde{y}_2}) m_Q^3 (e^{2\tilde{y}_2} + e^{\tilde{y}_1} (e^{\tilde{y}_1} - 2\xi) + 2e^{\tilde{y}_2} (e^{\tilde{y}_1} - 2\xi)) (e^{\tilde{y}_1} + e^{\tilde{y}_2} - 4\xi) \times \right. \\
& \left. \times (e^{2\tilde{y}_2} + e^{\tilde{y}_1} (e^{\tilde{y}_1} - 4\xi) + 2e^{\tilde{y}_2} (e^{\tilde{y}_1} - \xi)) (e^{\tilde{y}_1} + e^{\tilde{y}_2} + 2x - 2\xi) \right]^{-1}, \tag{B50}
\end{aligned}$$

$$\tilde{c}_4 = \frac{2e^{2\tilde{y}_1+\tilde{y}_2} (2e^{2\tilde{y}_1} + 2e^{2\tilde{y}_2} + 4e^{\tilde{y}_1+\tilde{y}_2} - 2e^{\tilde{y}_1}(x + \xi) - e^{\tilde{y}_2}(x + \xi))}{(e^{\tilde{y}_1} + e^{\tilde{y}_2})^2 m_Q^3 (e^{\tilde{y}_1} + e^{\tilde{y}_2} - 2(x + \xi)) (e^{2\tilde{y}_1} + e^{2\tilde{y}_2} + 2e^{\tilde{y}_1+\tilde{y}_2} - 2e^{\tilde{y}_1}(x + \xi) - e^{\tilde{y}_2}(x + \xi))}, \tag{B51}$$

$$\begin{aligned}
\tilde{c}_5 = & -\frac{2e^{2(\tilde{y}_1+\tilde{y}_2)}}{(e^{\tilde{y}_1} + e^{\tilde{y}_2})^2 m_Q^3 (e^{\tilde{y}_1} + e^{\tilde{y}_2} - 2(x + \xi))} \times \\
& \times \left( \frac{-4e^{2\tilde{y}_1}\xi - 4e^{2\tilde{y}_2}\xi - 8e^{\tilde{y}_1+\tilde{y}_2}\xi + 4e^{\tilde{y}_1}\xi(x + \xi) + 2e^{\tilde{y}_2}(x + \xi)(x + 3\xi)}{(e^{2\tilde{y}_2} + e^{\tilde{y}_1} (e^{\tilde{y}_1} - 2\xi) + 2e^{\tilde{y}_2} (e^{\tilde{y}_1} - 2\xi)) (e^{2\tilde{y}_1} + e^{2\tilde{y}_2} + 2e^{\tilde{y}_1+\tilde{y}_2} - e^{\tilde{y}_1}(x + \xi) - 2e^{\tilde{y}_2}(x + \xi))} + \right. \\
& \left. + \frac{(x + \xi) (e^{2\tilde{y}_2} + 2e^{\tilde{y}_2} (e^{\tilde{y}_1} - \xi) + e^{\tilde{y}_1} (e^{\tilde{y}_1} - 2(x + \xi)))}{(e^{2\tilde{y}_2} + e^{\tilde{y}_1} (e^{\tilde{y}_1} - 4\xi) + 2e^{\tilde{y}_2} (e^{\tilde{y}_1} - \xi)) (e^{2\tilde{y}_1} + e^{2\tilde{y}_2} + 2e^{\tilde{y}_1+\tilde{y}_2} - 2e^{\tilde{y}_1}(x + \xi) - e^{\tilde{y}_2}(x + \xi))} \right), \tag{B52}
\end{aligned}$$

$$\tilde{c}_6 = -\frac{2ie^{\tilde{y}_1+2\tilde{y}_2} (5(e^{\tilde{y}_1} + e^{\tilde{y}_2}) + 4(x + 4\xi))}{(e^{\tilde{y}_1} + e^{\tilde{y}_2})^2 m_Q^3 (e^{\tilde{y}_1} + e^{\tilde{y}_2} + 4\xi) (e^{\tilde{y}_1} + e^{\tilde{y}_2} + 2x + 6\xi)}, \tag{B53}$$

$$\begin{aligned}
\tilde{d}_1 = & 4e^{2\tilde{y}_2} Z (e^{\tilde{y}_1+2\tilde{y}_2} Q^2 - 4e^{\tilde{y}_1} m_Q^2 Z^2 + e^{\tilde{y}_2} (-e^{2\tilde{y}_1} Q^2 + 4m_Q^2 Z^2 + e^{\tilde{y}_1} Q^2(x - 2Z + \xi))) \times \\
& \times \left[ m_Q (-e^{2\tilde{y}_2} Q^2 + 2e^{\tilde{y}_2} Q^2 Z + 4m_Q^2 Z^2) (e^{\tilde{y}_2} - x - \xi) \times \right. \\
& \left. \times (e^{2\tilde{y}_2} (e^{\tilde{y}_1} Q^2 - 4m_Q^2 Z) - 4e^{\tilde{y}_1} m_Q^2 Z (e^{\tilde{y}_1} - x + Z - \xi) - 2e^{\tilde{y}_2} (e^{\tilde{y}_1} Q^2 - 4m_Q^2 Z) (e^{\tilde{y}_1} - x + Z - \xi)) \right]^{-1}, \tag{B54}
\end{aligned}$$

$$\tilde{d}_2 = \frac{8e^{2\tilde{y}_2} Z (e^{2\tilde{y}_2} Q^2 - 4m_Q^2 Z^2 - e^{\tilde{y}_2} Q^2(x + 2Z + \xi))}{m_Q (-e^{2\tilde{y}_2} Q^2 + 2e^{\tilde{y}_2} Q^2 Z + 4m_Q^2 Z^2) (e^{\tilde{y}_2} - x - \xi) (-e^{2\tilde{y}_2} Q^2 + 2e^{\tilde{y}_2} Q^2(x + Z + \xi) + 4m_Q^2 Z(x + Z + \xi))}. \tag{B55}$$

We may see that all the contributions, as a function of  $x$ , include poles; for this reason all the integrals which include convolution of these coefficient functions with GPDs should be understood in the principal value sense, taking into account the above-mentioned  $\xi \rightarrow \xi - i0$  prescription [34] for contour deformation near the poles. A special point of concern are the contributions  $c_1, c_2$ , which stem from the three-gluon diagrams 11-14 in Figure (3) and contain singularities  $\sim (x - \xi)^{-1}$ . These singularities apparently overlap with similar singularities in (B16), leading to the second-order poles. The integral in the vicinity of such singularities is defined via integration by parts [94],

$$\int_{-1}^1 dx \frac{H^g(x, \xi)}{(x \mp \xi \pm i0)^2} = -\int_{-1}^1 dx H^g(x, \xi) \frac{d}{dx} \left( \frac{1}{x \mp \xi \pm i0} \right) = -\frac{H^g(x, \xi)}{x \mp \xi \pm i0} \Big|_{-1}^1 + \int_{-1}^1 dx \frac{\partial_x H^g(x, \xi)}{x \mp \xi \pm i0} \tag{B56}$$

and exists only if the derivative  $\partial_x H^g(x, \xi)$  is a continuous function near the points  $x = \pm\xi$ . Fortunately, in the process under consideration such second-order poles cancel, since near the point  $x \approx \xi$  we have for residues

$$\text{Res}_{x=\xi} c_1 = -\text{Res}_{x=\xi} c_2. \quad (\text{B57})$$

A careful analysis demonstrates that such singularities occur only in the  $z_1 = z_2 = 1/2$  approximation. Beyond that limit, the two poles are separated from each other by a distance  $\pm \left(\frac{1}{4z_a} - z_a\right) e^{\tilde{y}_a}$  or an equivalent expression, which might be found by the replacement  $z_a \rightarrow 1 - z_a$ .

Finally, we need to mention that in the limit  $Q = 0$  it is possible to express the coefficients (B22-B55) in a compact form, as a function of skewedness variable  $\xi$  and rapidity difference  $\Delta y = y_1 - y_2$ . Since photoproduction gives the dominant contribution to the cross-section and might present special interest for future phenomenological studies, below we provide explicit expressions for this case:

$$a_5 = a_7 = b_1 = \tilde{a}_5 = \tilde{a}_7 = \tilde{b}_1 = 0 \quad (\text{B58})$$

$$a_1 = -\frac{2e^{2\Delta y}(\xi+1)(\xi+x)}{m_Q^3 (e^{\Delta y} + 1)^2 (2e^{\Delta y}(\xi+1) + 4\xi + 3) (\xi (e^{\Delta y}(\xi+1) + 2\xi + 1) - (e^{\Delta y} + 2)(\xi+1)x)} \quad (\text{B59})$$

$$a_2 = \frac{1}{m_Q^3 (e^{\Delta y} + 1)^2 (4\xi^2 + 7\xi + 3)} \quad (\text{B60})$$

$$a_3 = \frac{2e^{\Delta y} (2e^{\Delta y} + 1)}{m_Q^3 (e^{\Delta y} + 1)^2 (e^{\Delta y}(4\xi + 3) + 2(\xi + 1))} \quad (\text{B61})$$

$$a_4 = \frac{2e^{\Delta y}}{m_Q^3 (e^{\Delta y} + 1)^2 (4\xi + 3) (e^{\Delta y}(4\xi + 3) + 2(\xi + 1))} \quad (\text{B62})$$

$$a_6 = \frac{2e^{\Delta y} \xi^2}{m_Q^3 (e^{\Delta y} + 1)^2 (\xi(2\xi + 1) - 2(\xi + 1)x) (\xi (e^{\Delta y}(\xi + 1) + 2\xi + 1) - (e^{\Delta y} + 2)(\xi + 1)x)} \quad (\text{B63})$$

$$b_2 = \frac{\xi}{m_Q^3 (1 + \cosh(\Delta y)) (-\xi^2 + \xi x + x)} \quad (\text{B64})$$

$$b_3 = \frac{2e^{\Delta y} \xi^2}{m_Q^3 (e^{\Delta y} + 1)^2 (\xi^2 - (\xi + 1)x) (\xi(2\xi + 1) - 2(\xi + 1)x)} \quad (\text{B65})$$

$$c_1 = \frac{2e^{2\Delta y}}{(e^{\Delta y} + 1)^3 m_Q^3 (e^{\Delta y}(2\xi + 1) + 4\xi + 3) (e^{\Delta y}(4\xi + 3) + 2\xi + 1) (x - \xi) (\xi + 2(\xi^2 + \xi x + x))} \times \quad (\text{B66})$$

$$\times \left[ \xi^2 (-e^{2\Delta y}(2\xi + 1)(4\xi + 3) + 2e^{\Delta y}(2\xi(\xi + 4) + 5) - 2\xi(4\xi + 7) - 7) - 8(e^{\Delta y} - 1)(\xi + 1)^2 x^2 + 2e^{\Delta y} \xi x ((8\xi^2 + 4\xi - 1) \cosh(\Delta y) - 2(\xi + 1) \sinh(\Delta y) + 2\xi(5\xi + 4) + 1) \right]$$

$$c_2 = \frac{\text{sech}^2\left(\frac{\Delta y}{2}\right)}{2m_Q^3 (4\xi + 3)(x - \xi)(2(\xi + 1)x - \xi(2\xi + 1)) \left( (\xi + 1) \tanh\left(\frac{\Delta y}{2}\right) - 3\xi - 2 \right) \left( (\xi + 1) \tanh\left(\frac{\Delta y}{2}\right) + 3\xi + 2 \right)} \quad (\text{B67})$$

$$\times \left[ \frac{\xi ((4\xi + 3)(\sinh(\Delta y)(2\xi(2\xi + 1) - (4\xi + 3)x) + \cosh(\Delta y)(\xi(2\xi + 1) - 2(\xi + 1)x)) + \xi + 2(\xi + 1)(2\xi^2 + \xi x + x))}{\cosh(\Delta y) + 1} - 8(\xi + 1)^2 \sinh^4\left(\frac{\Delta y}{2}\right) \text{csch}^3(\Delta y) (\xi^2 - 2x^2) \right]$$

$$c_3 = \frac{2e^{2\Delta y} \xi ((2e^{\Delta y} + 1) (\xi^2 + \xi x + x) - \xi)}{(e^{\Delta y} + 1)^3 m_Q^3 (\xi + 2 (\xi^2 + \xi x + x)) (e^{\Delta y} (\xi + 2 (\xi^2 + \xi x + x)) + \xi^2 + \xi x + x)} \quad (\text{B68})$$

$$c_4 = \frac{(e^{\Delta y} + 1) (\xi + 1) \text{sech}^4 \left( \frac{\Delta y}{2} \right)}{8m_Q^3 (e^{\Delta y} (2\xi + 1) + 4\xi + 3) (e^{\Delta y} (4\xi + 3) + 2\xi + 1) (\xi + 2 (\xi^2 + \xi x + x)) ((e^{\Delta y} + 2) (\xi^2 + \xi x + x) + \xi)} \times \quad (\text{B69})$$

$$\times [e^{2\Delta y} (\xi^3 (60\xi^3 + 78\xi^2 + 32\xi + 5) + 2(\xi + 1)^2 x^3 + 2\xi(\xi + 1)(3\xi + 4)(10\xi + 7)x^2)$$

$$+ e^{2\Delta y} \xi^2 (2\xi(3\xi(20\xi + 43) + 83) + 31)x + e^{\Delta y} \xi^2 (2\xi(\xi(24\xi + 41) + 14) - 3)x$$

$$+ e^{\Delta y} (\xi^3 (\xi(12\xi(2\xi + 1) - 5) - 2) - 2(\xi + 1)^2 x^3 + \xi(\xi + 1)(4\xi(6\xi + 11) + 17)x^2)$$

$$+ (2\xi + 1) (-\xi^3 (2\xi(\xi + 4) + 3) + 2(\xi + 1)^2 x^3 + 2\xi(\xi + 1)^2 x^2 - \xi^2 (2\xi(\xi + 4) + 7)x$$

$$- e^{3\Delta y} (\xi^2 + \xi x + x) (-\xi(14\xi + 11) + 2\xi x + x) (\xi + 2 (\xi^2 + \xi x + x))] (\xi e^{\Delta y} + (\xi^2 + \xi x + x) (1 + 2e^{\Delta y}))^{-1}$$

$$c_5 = \frac{4e^{\Delta y} (\xi(16\xi + 21) + 4(\xi + 1)x)}{(e^{\Delta y} + 1)^3 m_Q^3 (4\xi + 5)(\xi(6\xi + 7) + 2(\xi + 1)x)} \quad (\text{B70})$$

$$d_1 = \frac{4\xi^2 \sinh \left( \frac{\Delta y}{2} \right) \left( \cosh \left( \frac{\Delta y}{2} \right) (\xi + 2 (\xi^2 + \xi x + x)) - \xi \sinh \left( \frac{\Delta y}{2} \right) \right)^{-1}}{m_Q^3 (-3 \sinh(\Delta y) (3\xi^2 + \xi(x + 2) + x) + \cosh(\Delta y) (3\xi^2 + \xi(x + 4) + x) + 3\xi^2 + \xi x + x)} \quad (\text{B71})$$

$$d_2 = -\frac{2e^{\Delta y} \xi^2}{m_Q^3 (e^{\Delta y} + 1) (-\xi^2 + \xi x + x) ((e^{\Delta y} + 1) (\xi^2 + \xi x + x) + \xi)} \quad (\text{B72})$$

$$\tilde{a}_1 = \frac{2e^{2\Delta y} (\xi + 1) (\xi + x)}{m_Q^3 (e^{\Delta y} + 1)^2 (2e^{\Delta y} (\xi + 1) + 4\xi + 3) (\xi (e^{\Delta y} (\xi + 1) + 2\xi + 1) - (e^{\Delta y} + 2) (\xi + 1)x)} \quad (\text{B73})$$

$$\tilde{a}_2 = -\frac{1}{m_Q^3 (e^{\Delta y} + 1)^2 (4\xi^2 + 7\xi + 3)} \quad (\text{B74})$$

$$\tilde{a}_3 = \frac{2e^{\Delta y} (2e^{\Delta y} + 1)}{m_Q^3 (e^{\Delta y} + 1)^2 (e^{\Delta y} (4\xi + 3) + 2(\xi + 1))} \quad (\text{B75})$$

$$\tilde{a}_4 = -\frac{2e^{\Delta y}}{m_Q^3 (e^{\Delta y} + 1)^2 (4\xi + 3) (e^{\Delta y} (4\xi + 3) + 2(\xi + 1))} \quad (\text{B76})$$

$$\tilde{a}_6 = -\frac{\xi^2}{m_Q^3 (\cosh(\Delta y) + 1) (\xi(2\xi + 1) - 2(\xi + 1)x) (\xi (e^{\Delta y} (\xi + 1) + 2\xi + 1) - (e^{\Delta y} + 2) (\xi + 1)x)} \quad (\text{B77})$$

$$\tilde{b}_2 = -\frac{\xi}{m_Q^3 (\cosh(\Delta y) + 1) (-\xi^2 + \xi x + x)} \quad (\text{B78})$$

$$\tilde{b}_3 = -\frac{\xi^2}{m_Q^3 (\cosh(\Delta y) + 1) (-\xi^2 + \xi x + x) (2(\xi + 1)x - \xi(2\xi + 1))} \quad (\text{B79})$$

$$\tilde{c}_1 = \frac{2e^{2\Delta y} (\xi (e^{2\Delta y} (2\xi + 1)(4\xi + 3) + 2e^{\Delta y} (5\xi(2\xi + 3) + 6) - 4\xi(\xi + 3) - 7) + 8(e^{\Delta y} - 1) (\xi + 1)^2 x)}{m_Q^3 (e^{\Delta y} + 1)^3 (e^{\Delta y} (2\xi + 1) + 4\xi + 3) (e^{\Delta y} (4\xi + 3) + 2\xi + 1) (\xi + 2 (\xi^2 + \xi x + x))} \quad (\text{B80})$$

$$\tilde{c}_2 = -\frac{2e^{\Delta y}}{m_Q^3 (e^{\Delta y} + 1)^3 (4\xi + 3) (e^{\Delta y}(2\xi + 1) + 4\xi + 3) (e^{\Delta y}(4\xi + 3) + 2\xi + 1) (\xi(2\xi + 1) - 2(\xi + 1)x)} \times \quad (\text{B81})$$

$$\times [e^{3\Delta y}\xi(2\xi + 1)(4\xi + 3) - e^{\Delta y}(-4(2\xi + 1)\xi^2 + \xi + 8(\xi + 1)(3\xi + 2)x) + e^{2\Delta y}(3\xi(2\xi + 1)^2 - 8(\xi + 1)(3\xi + 2)x) + \xi(2\xi + 1)(4\xi + 3)]$$

$$\tilde{c}_3 = -\frac{\text{sech}^4\left(\frac{\Delta y}{2}\right)}{2m_Q^3(4\xi + 3)(\xi(2\xi + 1) - 2(\xi + 1)x) \left((\xi + 1)\tanh\left(\frac{\Delta y}{2}\right) - 3\xi - 2\right) \left((\xi + 1)\tanh\left(\frac{\Delta y}{2}\right) + 3\xi + 2\right)} \times \quad (\text{B82})$$

$$\times \left(-\xi(\xi + 1)^2 \tanh\left(\frac{\Delta y}{2}\right) + (2\xi + 1)\cosh(\Delta y)(-3\xi^2 + \xi(x - 2) + x) - \xi(3\xi + 2)(4\xi + 3) + (\xi + 1)^2 x\right) \quad (\text{B83})$$

$$\tilde{c}_4 = \frac{2e^{2\Delta y}\xi((2e^{\Delta y} + 1)(\xi^2 + \xi x + x) - \xi)}{m_Q^3 (e^{\Delta y} + 1)^3 (\xi + 2(\xi^2 + \xi x + x))(e^{\Delta y}(\xi + 2(\xi^2 + \xi x + x)) + \xi^2 + \xi x + x)} \quad (\text{B84})$$

$$\tilde{c}_5 = -\frac{(e^{\Delta y} + 1)(\xi + 1)\text{sech}^4\left(\frac{\Delta y}{2}\right)(\xi e^{\Delta y} + (\xi^2 + \xi x + x)(1 + 2e^{\Delta y}))^{-1}}{8m_Q^3 (e^{\Delta y}(2\xi + 1) + 4\xi + 3) (e^{\Delta y}(4\xi + 3) + 2\xi + 1) (\xi + 2(\xi^2 + \xi x + x)) ((e^{\Delta y} + 2)(\xi^2 + \xi x + x) + \xi)} \times \quad (\text{B85})$$

$$\times \left[ e^{2\Delta y}(\xi^3(60\xi^3 + 78\xi^2 + 32\xi + 5) + 2(\xi + 1)^2 x^3 + 2\xi(\xi + 1)(3\xi + 4)(10\xi + 7)x^2) \right. \\ + e^{\Delta y}(\xi^3(\xi(12\xi(2\xi + 1) - 5) - 2) - 2(\xi + 1)^2 x^3 + \xi(\xi + 1)(4\xi(6\xi + 11) + 17)x^2) \\ + x\xi^2 e^{2\Delta y}(2\xi(3\xi(20\xi + 43) + 83) + 31) + x\xi^2 e^{\Delta y}(2\xi(\xi(24\xi + 41) + 14) - 3) \\ + (2\xi + 1)(-\xi^3(2\xi(\xi + 4) + 3) + 2(\xi + 1)^2 x^3 + 2\xi(\xi + 1)^2 x^2 - \xi^2(2\xi(\xi + 4) + 7)x) \\ \left. - e^{3\Delta y}(\xi^2 + \xi x + x)(-\xi(14\xi + 11) + 2\xi x + x)(\xi + 2(\xi^2 + \xi x + x)) \right] \quad (\text{B86})$$

$$\tilde{c}_6 = -\frac{4e^{\Delta y}(\xi(16\xi + 21) + 4(\xi + 1)x)}{m_Q^3 (e^{\Delta y} + 1)^3 (4\xi + 5)(\xi(6\xi + 7) + 2(\xi + 1)x)} \quad (\text{B87})$$

$$\tilde{d}_1 = \frac{2(e^{\Delta y} - 1)\xi^2(e^{\Delta y}(\xi + 1)(\xi + x) + \xi^2 + \xi x + x)^{-1}}{m_Q^3 (\xi(-3e^{\Delta y}\xi + e^{2\Delta y}(3\xi + 1) - 6\xi - 5) + (e^{\Delta y} - 2)(e^{\Delta y} + 1)(\xi + 1)x)} \quad (\text{B88})$$

$$\tilde{d}_2 = \frac{2\xi^2}{m_Q^3 (e^{\Delta y} + 1)(-\xi^2 + \xi x + x)(e^{\Delta y}(\xi + 1)(\xi + x) + \xi^2 + \xi x + x)} \quad (\text{B89})$$

- 
- [1] M. Diehl, T. Feldmann, R. Jakob and P. Kroll, Nucl. Phys. B **596**, 33 (2001) [Erratum-ibid. B **605**, 647 (2001)] [arXiv:hep-ph/0009255].
- [2] K. Goetze, M. V. Polyakov and M. Vanderhaeghen, Prog. Part. Nucl. Phys. **47**, 401 (2001) [arXiv:hep-ph/0106012].
- [3] M. Diehl, Phys. Rept. **388**, 41 (2003) [arXiv:hep-ph/0307382].
- [4] M. Guidal, H. Moutarde and M. Vanderhaeghen, “Generalized Parton Distributions in the valence region from Deeply Virtual Compton Scattering,” Rept. Prog. Phys. **76** (2013), 066202 [arXiv:1303.6600 [hep-ph]].
- [5] D. Boer, M. Diehl, R. Milner, R. Venugopalan, W. Vogelsang, D. Kaplan, H. Montgomery, S. Vigdor, A. Accardi and E. C. Aschenauer, *et al.* “Gluons and the quark sea at high energies: Distributions, polarization, tomography,” [arXiv:1108.1713 [nucl-th]].
- [6] V. Burkert, L. Elouadrhiri, A. Afanasev, J. Arrington, M. Contalbrigo, W. Cosyn, A. Deshpande, D. Glazier, X. Ji and S. Liuti, *et al.* “Precision Studies of QCD in the Low Energy Domain of the EIC,” [arXiv:2211.15746 [nucl-ex]].
- [7] K. Kumericki, S. Liuti and H. Moutarde, “GPD phenomenology and DVCS fitting: Entering the high-precision era,” Eur. Phys. J. A **52** (2016) no.6, 157 [arXiv:1602.02763 [hep-ph]].



- [8] G. Duplanić, S. Nabeebaccus, K. Passek-Kumerički, B. Pire, L. Szymanowski and S. Wallon, “*Accessing chiral-even quark generalised parton distributions in the exclusive photoproduction of a  $\gamma\pi^\pm$  pair with large invariant mass in both fixed-target and collider experiments*,” [arXiv:2212.00655 [hep-ph]].
- [9] G. Duplanić, K. Passek-Passek-Kumerički, B. Pire, L. Szymanowski and S. Wallon, JHEP 11 (2018) 179 [arXiv:1809.08104 [hep-ph]].
- [10] R. Boussarie, B. Pire, L. Szymanowski and S. Wallon, JHEP 02 (2017) 054 [arXiv:1609.03830 [hep-ph]].
- [11] W. Cosyn and B. Pire, Phys. Rev. D 103 (2021) 114002 [arXiv:2103.01411 [hep-ph]].
- [12] A. Pedrak, B. Pire, L. Szymanowski and J. Wagner, Phys. Rev. D 101 (2020) 114027 [arXiv:2003.03263 [hep-ph]].
- [13] B. Pire, L. Szymanowski and S. Wallon, Phys. Rev. D 101 (2020) 074005 [arXiv:1912.10353 [hep-ph]].
- [14] A. Pedrak, B. Pire, L. Szymanowski and J. Wagner, Phys. Rev. D 96 (2017) 074008 [arXiv:1708.01043 [hep-ph]].
- [15] M. El Beiyad, B. Pire, M. Segond, L. Szymanowski and S. Wallon, Phys. Lett. B 688 (2010) 154 [arXiv:1001.4491 [hep-ph]].
- [16] D.Y. Ivanov, B. Pire, L. Szymanowski and O.V. Teryaev, Phys. Lett. B 550 (2002) 65 [arXiv:hep-ph/0209300].
- [17] G. Duplanić, S. Nabeebaccus, K. Passek-Kumerički, B. Pire, L. Szymanowski and S. Wallon, “*Accessing GPDs through the exclusive photoproduction of a photon-meson pair with a large invariant mass*,” [arXiv:2212.01034 [hep-ph]].
- [18] J.-W. Qiu and Z. Yu, “*Exclusive production of a pair of high transverse momentum photons in pion-nucleon collisions for extracting generalized parton distributions*”, [arXiv:2205.07846 [hep-ph]].
- [19] J.-W. Qiu and Z. Yu, “*Single diffractive hard exclusive processes for the study of generalized parton distributions*”, [arXiv:2210.07995 [hep-ph]].
- [20] J. G. Körner and G. Thompson, Phys. Lett. B 264, 185 (1991).
- [21] M. Neubert, “*Heavy quark symmetry*,” Phys. Rept. 245 (1994), 259-396 [arXiv:hep-ph/9306320 [hep-ph]].
- [22] G. T. Bodwin, E. Braaten and G. P. Lepage, Phys. Rev. D 51, 1125 (1995) Erratum: [Phys. Rev. D 55, 5853 (1997)] [hep-ph/9407339].
- [23] F. Maltoni, M. L. Mangano and A. Petrelli, Nucl. Phys. B 519, 361 (1998) [hep-ph/9708349].
- [24] N. Brambilla, A. Vairo and E. Mereghetti, Phys. Rev. D 79, 074002 (2009) Erratum: [Phys. Rev. D 83, 079904 (2011)] [arXiv:0810.2259 [hep-ph]].
- [25] Y. Feng, J. P. Lansberg and J. X. Wang, Eur. Phys. J. C 75, no. 7, 313 (2015) [arXiv:1504.00317 [hep-ph]].
- [26] N. Brambilla *et al.*; Eur. Phys. J. C 71, 1534 (2011).
- [27] P. L. Cho and A. K. Leibovich, Phys. Rev. D 53, 6203 (1996) [hep-ph/9511315].
- [28] P. L. Cho and A. K. Leibovich, Phys. Rev. D 53, 150 (1996) [hep-ph/9505329].
- [29] S. P. Baranov, Phys. Rev. D 66, 114003 (2002).
- [30] S. P. Baranov and A. Szczurek, Phys. Rev. D 77, 054016 (2008) [arXiv:0710.1792 [hep-ph]].
- [31] S. P. Baranov, A. V. Lipatov and N. P. Zotov, Phys. Rev. D 85, 014034 (2012) [arXiv:1108.2856 [hep-ph]].
- [32] S. P. Baranov and A. V. Lipatov, Phys. Rev. D 96, no. 3, 034019 (2017) [arXiv:1611.10141 [hep-ph]].
- [33] S.P. Baranov, A.V. Lipatov, N.P. Zotov; Eur. Phys. J. C 75, 455 (2015).
- [34] D.Yu. Ivanov, A. Schafer, L. Szymanowski and G. Krasnikov, Eur. Phys. J. C 34 (2004) 297, [arXiv:hep-ph/0401131].
- [35] M. Vanttinen and L. Mankiewicz, Phys. Lett. B 440 (1998) 157, [arXiv:hep-ph/9807287].
- [36] J. Koempel, P. Kroll, A. Metz and J. Zhou, Phys. Rev. D 85 (2012) 051502(R) [arXiv:1112.1334 [hep-ph]].
- [37] Z.L. Cui, M.C. Hu and J.P. Ma, Eur. Phys. J. C 79 (2019), 812 [arXiv:1804.05293 [hep-ph]].
- [38] S. J. Brodsky, G. Kopp and P. M. Zerwas, “*Hadron Production Near Threshold in Photon-photon Collisions*,” Phys. Rev. Lett. 58 (1987), 443.
- [39] G. P. Lepage and S. J. Brodsky, “*Exclusive processes in perturbative quantum chromodynamics*”, Phys. Rev. D 22 (1980) 2157.
- [40] C. Berger and W. Wagner, “*Photon-Photon Reactions*,” Phys. Rept. 146 (1987), 1-134.
- [41] M. S. Baek, S. Y. Choi and H. S. Song, “*Exclusive heavy meson pair production at large recoil*,” Phys. Rev. D 50 (1994), 4363-4371.
- [42] Y. Bai, S. Lu and J. Osborne, arXiv:1612.00012 [hep-ph].
- [43] W. Heupel, G. Eichmann and C. S. Fischer, Phys. Lett. B 718, 545 (2012) [arXiv:1206.5129 [hep-ph]].
- [44] R. J. Lloyd and J. P. Vary, Phys. Rev. D 70, 014009 (2004) [hep-ph/0311179].
- [45] J. Vijande, N. Barnea and A. Valcarce, Int. J. Mod. Phys. A 22, 561 (2007) [hep-ph/0610124].
- [46] J. Vijande, A. Valcarce and J.-M. Richard, Few Body Syst. 54, 1015 (2013) [arXiv:1212.4273 [hep-ph]].
- [47] X. Chen, “*Fully-heavy tetraquarks:  $bb\bar{c}$  and  $b\bar{c}\bar{c}$* ,” Phys. Rev. D 100 (2019) no.9, 094009 [arXiv:1908.08811 [hep-ph]].
- [48] A. Esposito and A. D. Polosa, “*A  $bb\bar{b}\bar{b}$  di-bottomonium at the LHC*,” Eur. Phys. J. C 78 (2018) no.9, 782 [arXiv:1807.06040 [hep-ph]].
- [49] R. Cardinale [LHCb], “*LHCb spectroscopy results*,” PoS LHCP2018 (2018), 191
- [50] R. Aaij *et al.* [LHCb], “*Search for beautiful tetraquarks in the  $\Upsilon(1S)\mu^+\mu^-$  invariant-mass spectrum*,” JHEP 10 (2018), 086 [arXiv:1806.09707 [hep-ex]].
- [51] L. Capriotti [LHCb], “*Spectroscopy of Heavy Hadrons at LHCb*,” J. Phys. Conf. Ser. 1137 (2019) no.1, 012004
- [52] R. Aaij *et al.* [LHCb], “*Observation of structure in the  $J/\psi$  -pair mass spectrum*,” Sci. Bull. 65 (2020) no.23, 1983-1993 [arXiv:2006.16957 [hep-ex]].
- [53] V. P. Goncalves, B. D. Moreira and F. S. Navarra, “*Double vector meson production in  $\gamma\gamma$  interactions at hadronic colliders*,” Eur. Phys. J. C 76 (2016) no.3, 103 [arXiv:1512.07482 [hep-ph]].
- [54] V.P. Goncalves and R. Palota da Silva, “*Exclusive and diffractive quarkonium - pair production at the LHC and FCC*,” Phys. Rev. D 101 (2020) no.3, 034025 [arXiv:1912.02720 [hep-ph]].
- [55] V. P. Goncalves and M. V. T. Machado, “*Dipole model for double meson production in two-photon interactions at high*

- energies,” Eur. Phys. J. C **49** (2007), 675-684 [arXiv:hep-ph/0605304 [hep-ph]].
- [56] S. Baranov, A. Cisek, M. Klusek-Gawenda, W. Schafer and A. Szczurek, “*The  $\gamma\gamma \rightarrow J/\psi J/\psi$  reaction and the  $J/\psi J/\psi$  pair production in exclusive ultraperipheral ultrarelativistic heavy ion collisions*,” Eur. Phys. J. C **73** (2013) no.2, 2335 [arXiv:1208.5917 [hep-ph]].
- [57] H. Yang, Z. Q. Chen and C. F. Qiao, “*NLO QCD corrections to exclusive quarkonium-pair production in photon-photon collision*,” Eur. Phys. J. C **80** (2020) no.9, 806.
- [58] V. P. Goncalves, B. D. Moreira and F. S. Navarra, “*Double vector meson production in photon-hadron interactions at hadronic colliders*,” Eur. Phys. J. C **76** (2016) no.7, 388 [arXiv:1605.05840 [hep-ph]].
- [59] S. Andradé, M. Siddikov and I. Schmidt, “*Exclusive photoproduction of heavy quarkonia pairs*,” [arXiv:2202.03288 [hep-ph]].
- [60] A. Accardi *et al.*, Eur. Phys. J. C **52**, no. 9, 268 (2016) [arXiv:1212.1701 [nucl-ex]].
- [61] Press release at the website of the United States Department of Energy: <https://www.energy.gov/articles/us-department-energy-selects-brookhaven-national-laboratory-host-major-new-nuclear-physics>.
- [62] Press-release at the website of the Brookhaven National Laboratory (BNL): <https://www.bnl.gov/newsroom/news.php?a=116998>.
- [63] R. Abdul Khalek *et al.* “*Science Requirements and Detector Concepts for the Electron-Ion Collider: EIC Yellow Report*,” [arXiv:2103.05419 [physics.ins-det]].
- [64] B. Lehmann-Dronke, P. V. Pobylitsa, M. V. Polyakov, A. Schafer and K. Goetze, “*Hard diffractive electroproduction of two pions*,” Phys. Lett. B **475** (2000), 147-156 [arXiv:hep-ph/9910310 [hep-ph]].
- [65] B. Lehmann-Dronke, A. Schafer, M. V. Polyakov and K. Goetze, “*Angular distributions in hard exclusive production of pion pairs*,” Phys. Rev. D **63** (2001), 114001 [arXiv:hep-ph/0012108 [hep-ph]].
- [66] B. Clerbaux and M. V. Polyakov, “*Partonic structure of pi and rho mesons from data on hard exclusive production of two pions off nucleon*,” Nucl. Phys. A **679** (2000), 185-195 [arXiv:hep-ph/0001332 [hep-ph]].
- [67] M. Diehl, T. Gousset and B. Pire, “*Polarization in deeply virtual meson production*,” [arXiv:hep-ph/9909445 [hep-ph]].
- [68] J. Breitweg *et al.* [ZEUS], “*Exclusive electroproduction of  $\rho^0$  and  $J/\psi$  mesons at HERA*,” Eur. Phys. J. C **6** (1999), 603-627 [arXiv:hep-ex/9808020 [hep-ex]].
- [69] A. V. Radyushkin, Phys. Lett. B **380**, 417 (1996) [arXiv:hep-ph/9604317].
- [70] A. V. Radyushkin, Phys. Rev. D **56**, 5524 (1997).
- [71] J. C. Collins and A. Freund, Phys. Rev. D **59**, 074009 (1999).
- [72] X. D. Ji, Phys. Rev. D **55**, 7114 (1997).
- [73] X. D. Ji and J. Osborne, Phys. Rev. D **58** (1998) 094018 [arXiv:hep-ph/9801260].
- [74] A. V. Belitsky, D. Mueller and A. Kirchner, Nucl. Phys. B **629**, 323 (2002) [arXiv:hep-ph/0112108].
- [75] A. V. Belitsky and A. V. Radyushkin, Phys. Rept. **418**, 1 (2005) [arXiv:hep-ph/0504030].
- [76] S. V. Goloskokov and P. Kroll, Eur. Phys. J. C **50**, 829 (2007) [hep-ph/0611290].
- [77] S. V. Goloskokov and P. Kroll, Eur. Phys. J. C **53**, 367 (2008) [arXiv:0708.3569 [hep-ph]].
- [78] S. V. Goloskokov and P. Kroll, Eur. Phys. J. C **59** (2009) 809 [arXiv:0809.4126 [hep-ph]].
- [79] S. V. Goloskokov and P. Kroll, Eur. Phys. J. C **65**, 137 (2010) [arXiv:0906.0460 [hep-ph]].
- [80] S. V. Goloskokov and P. Kroll, Eur. Phys. J. A **47**, 112 (2011) [arXiv:1106.4897 [hep-ph]].
- [81] S. V. Goloskokov and P. Kroll, “*Transversity in exclusive vector-meson leptoproduction*,” Eur. Phys. J. C **74** (2014), 2725 [arXiv:1310.1472 [hep-ph]].
- [82] S. J. Brodsky, H. C. Pauli and S. S. Pinsky, “*Quantum chromodynamics and other field theories on the light cone*,” Phys. Rept. **301** (1998), 299-486 [arXiv:hep-ph/9705477 [hep-ph]].
- [83] X. D. Ji, J. Phys. G **24**, 1181 (1998) [arXiv:hep-ph/9807358].
- [84] E. Braaten and J. Lee, “*Exclusive Double Charmonium Production from  $e^+e^-$  Annihilation into a Virtual Photon*,” Phys. Rev. D **67** (2003), 054007 [erratum: Phys. Rev. D **72** (2005), 099901] [arXiv:hep-ph/0211085 [hep-ph]].
- [85] M. El Beiyad, B. Pire, M. Segond, L. Szymanowski and S. Wallon, “*Photoproduction of a pi rhoT pair with a large invariant mass and transversity generalized parton distribution*,” Phys. Lett. B **688** (2010), 154-167 [arXiv:1001.4491 [hep-ph]].
- [86] R. Boussarie, B. Pire, L. Szymanowski and S. Wallon, “*Exclusive photoproduction of a  $\gamma \rho$  pair with a large invariant mass*,” JHEP **02** (2017), 054 [erratum: JHEP **10** (2018), 029] [arXiv:1609.03830 [hep-ph]].
- [87] B. Pire and L. Szymanowski, “*Neutrino-production of a charmed meson and the transverse spin structure of the nucleon*,” Phys. Rev. Lett. **115** (2015) no.9, 092001 [arXiv:1505.00917 [hep-ph]].
- [88] B. Pire and L. Szymanowski, “*Exclusive neutrino production of a charmed vector meson and transversity gluon generalized parton distributions*,” Phys. Rev. D **96** (2017) no.11, 114008 [arXiv:1711.04608 [hep-ph]].
- [89] B. Pire, L. Szymanowski and J. Wagner, “*Exclusive neutrino-production of a charmed meson*,” Phys. Rev. D **95** (2017) no.9, 094001 [arXiv:1702.00316 [hep-ph]].
- [90] B. Pire, L. Szymanowski and J. Wagner, “*Charged current electroproduction of a charmed meson at an electron-ion collider*,” Phys. Rev. D **104** (2021) no.9, 094002 [arXiv:2104.04944 [hep-ph]].
- [91] V. Shtabovenko, R. Mertig and F. Orellana, Comput. Phys. Commun., 207, 432-444, 2016, arXiv:1601.01167.
- [92] R. Mertig, M. Böhm, and A. Denner, Comput. Phys. Commun., 64, 345-359, 1991.
- [93] M. Butenschoen, Z. G. He and B. A. Kniehl, “ *$\eta_c$  production at the LHC challenges nonrelativistic-QCD factorization*,” Phys. Rev. Lett. **114** (2015) no.9, 092004 [arXiv:1411.5287 [hep-ph]].
- [94] S. P. Baranov, “*Diffractive open charm production at DESY HERA: Experiment versus two-gluon exchange model*,” Phys. Rev. D **81** (2010), 034021.